Schweizerische Eidgenossenschaft
Confédération suisse
Confederazione Svizzera
Confederaziun svizra

Eidgenössisches Departement für Umwelt, Verkehr, Energie und Kommunikation UVEK
Département fédéral de l'environnement, des transports, de l'énergie et de la communication DETEC
Dipartimento federale dell'ambiente, dei trasporti, dell'energia e delle comunicazioni DATEC

Bundesamt für Strassen
Office fédéral des routes
Ufficio federale delle Strade

Strengthening of bridge deck slabs with textile reinforced concrete

Verstärken von Fahrbahnplatten mit Textilbeton

Renforcement de dalles de roulement avec le béton armé aux textiles

Haute école spécialisée de Suisse occidentale (HES-SO)
Haute école d'ingénierie at d'architecture Fribourg (HEIA-FR)
Institut des Technologies de l'Environnement Construit (iTEC)

Alex-Manuel Muresan, MSc civil eng.
Prof. Dr. Daia Zwicky, dipl. Bauing. ETH

Research project AGB 2015/005 upon application of the Working Group for Bridge Research (AGB)

June 2021 **702**

Impressum

Forschungsstelle und Projektteam
Projektleitung
Prof. Dr. Daia Zwicky, iTEC / HEIA-FR / HES-SO

Mitglieder
Alex-Manuel Mureşan, iTEC / HEIA-FR / HES-SO
Marco Maeder, iTEC / HEIA-FR / HES-SO

Begleitkommission
Präsident
Jean-Christophe Putallaz

Mitglieder
Stéphane Cuennet
Herbert Friedl
Dr. Pascal Kronenberg
Prof. Dr. Aurelio Muttoni
Dr. Ana Spasojevic

KO-Finanzierung des Forschungsprojekts
Haute Ecole Spécialisée de la Suisse Occidentale (HES-SO)
Master en Ingénierie du Territoire (MIT)

Antragsteller
Arbeitsgruppe Brückenforschung (AGB)

Bezugsquelle
Das Dokument kann kostenlos von http://www.mobilityplatform.ch heruntergeladen werden.

Table of contents

Impressum **4**
Zusammenfassung **7**
Résumé **11**
Summary **13**

1 Introduction **15**

2 Basic materials **17**
2.1 Textile reinforcement 17
2.1.1 General description and production process of reinforcement textiles 17
2.1.2 Usual geometries of yarn and mesh 17
2.1.3 Mechanical properties and behavior of fibers 18
2.2 Mortar matrix 19
2.2.1 Mechanical properties and behavior 20
2.2.2 Long-term behavior 20

3 Mechanical behavior of textile reinforced concrete **21**
3.1 Experimental observations 21
3.2 Bond capacity 22
3.2.1 Bond behavior of a single yarn – Mobasher's model 23
3.2.2 Bond behavior of multiple yarns – Maeder's dimensioning model 26
3.2.3 Experimental study 26
3.2.4 Model parameter value calibration 28
3.2.5 Influence of bond width 29
3.2.6 Dimensioning model 33
3.3 Mechanical anchorage 35
3.4 Interface between TRC and concrete support 35

4 Database evaluation for suitability of analytical dimensioning approaches **37**
4.1 Database 37
4.2 Empirical evaluation 37
4.3 Suitability evaluation of structural analysis approaches 38
4.3.1 Rigid bond approach 38
4.3.2 Unbonded end-anchored textile reinforcement 39
4.3.3 Anchorage length for strengthening textile 40
4.3.4 Cracked length 41
4.3.5 Length with yielding steel reinforcement 42
4.3.6 Ultimate deflection in unbonded end-anchored approach 44
4.3.7 Friction coefficient approach 45
4.3.8 Bond coefficients approach 46

5 Proposal for flexural strengthening design of one-way slabs with TRC **47**
5.1 Strain limit approach 47
5.2 Structural analysis and dimensioning 49
5.2.1 Sectional analysis 49
5.2.2 Characteristic and design values 50

6 Conclusion **53**

7 Further research needs and practical implication **55**

Glossary **56**
References **58**
Project closure **61**

Zusammenfassung

Dieser Bericht zeigt die Resultate einer Eignungsprüfung von verschiedenen theoretischen Ansätzen für die Bemessung der Biegeverstärkung von Fahrbahnplatten mit sogenanntem textilbewehrtem Feinkornbeton («Textilbeton») im Grenzzustand der Tragsicherheit.

Textilbeton ist ein Verbundwerkstoff, der die hohe Zugfestigkeit von Kunstfasertextilien mit der Verbundwirkung und dem mechanischen und thermischen Schutz von Feinkornbeton (d.h. Zementmörteln) vereint. Neben seiner Anwendung in der Herstellung von neuen Bauteilen wird Textilbeton auch als Verstärkungsmassnahme für bestehende Bauteile aus Stahlbeton eingesetzt. In dieser Anwendung basieren die am häufigsten verwendeten Textilien auf Carbon-, Basalt- oder PBO-Fasern (Poly-Phenylen-2,6-Benzobisoxazol, auch bekannt als Zylon), seltener werden auch Glasfaserbasierte Textilien eingesetzt. Solche Fasern werden mittels Kunstharz (meist Epoxy) in hochfesten Garnen gebündelt, welche zu Textilien verwoben werden, die für die Anwendung im Neubau und in Verstärkungen i.d.R. als Bewehrungsgitter eingesetzt werden.

Die geometrischen Eigenschaften der Textilgitter variieren stark von Anbieter zu Anbieter. Der Garnabstand ist üblicherweise zwischen 10 mm und 40 mm, kann aber auch nur 5 mm betragen. Die Garne haben elliptische bis runde Querschnitte mit Verhältnissen der Durchmesser von 1 (Kreis) bis 10 (sehr flache Ellipse). Die Querschnittsfläche der einzelnen Garne variiert ebenfalls sehr stark, und kann je nach Anbieter etwa 0.2 mm^2 bis zu 3 mm^2 betragen. Dank ihrer dünnen Geometrie sind Textilgitter sehr biegeweich und sehr leicht. Sie können daher in grossen Längen hergestellt, gerollt transportiert und einfach eingebaut werden. Sie können zudem mit einfachen Hilfsmitteln auf der Baustelle auf die erforderliche Länge zugeschnitten werden.

Das mechanische Verhalten der Textilgarne ist quasi-spröd, d.h. linear elastisch bis zum Bruch. PBO-Fasern weisen mit einem Elastizitätsmodul von 270-280 GPa und einer Zugfestigkeit von 5’800-6'000 MPa die höchsten mechanischen Eigenschaften auf. Carbonfasern zeigen mit 240 GPa resp. 4’300 MPa etwas geringere Werte. Basalt- und Glasfasern haben mit einem E-Modul von 80-90 GPa und einer Zugfestigkeit von 2'600-3'000 MPa deutlich tiefere mechanische Eigenschaften. Infolge der Verbundwirkung mit dem umgebenden Feinkornbeton, aber auch wegen der nie vollständigen Tränkung der Garne mit Kunstharz können die hohen Zugfestigkeiten der Fasern eh kaum ausgenützt werden. Hingegen verändern sich ihre mechanischen Eigenschaften nicht signifikant über die Zeit, die Textilien sind sehr dauerhaft. Für Carbonfasern besteht bei Temperaturen von über etwa 300°C die Gefahr von Oxidation (Transformation von Carbon in CO_2). Der von der Überdeckung aus Feinkornbeton zur Verfügung gestellte Brandschutz ist üblicherweise aber ausreichend hoch, um genügend lange Brandwiderstandsdauern zu erreichen. Dies ist gegenüber extern angebrachten Klebebewehrungen aus faserverstärkten Polymeren, bei denen die Klebstoffe bei ca. 80°C verspröden und brechen, ein wesentlicher Vorteil von Textilbeton.

Der Feinkornbeton stellt neben diesem Brandschutz insbesondere den erforderlichen Verbund – und damit auch die Endverankerung – für die Textilgitter zur Verfügung. Zudem ergänzt der Feinkornbeton die Betonüberdeckung einer im bestehenden Betonbauteil vorhandenen Stahlbewehrung und erhöht damit deren Korrosionsschutz. Er stellt ebenfalls die Endverankerung der Textilien mittels Verbund zur Verfügung. Diese wurde im Rahmen einer Versuchsreihe vertieft untersucht, die – neben weiteren Daten aus der Literatur – als Grundlage für die Kalibrierung von Parameterwerten eines bestehenden Verbundmodells am Einzelgarn diente. Daraus wurde ein Vorschlag abgeleitet für die Bemessung von Verbundverankerungen von in Feinkornbeton eingebetteten Textilgarnen. Diese Verankerungen sollten sich – wie bei Klebebewehrungen – im ungerissen bleibenden Bereich des Stahlbetonbauteils befinden. Die benötigten Verankerungslängen hängen im Wesentlichen von der Textilgeometrie und den Feinkornbetoneigenschaften ab und befinden sich üblicherweise im tiefen zweistelligen Zentimeterbereich. Weitere Details zur Versuchsreihe und zum Bemessungsvorschlag finden sich in diesem Bericht.

Das Tragverhalten des Verbundwerkstoffs Textilbeton auf Zug ist multi-linear und zeichnet sich durch drei Phasen aus. In einer ersten ungerissenen Phase trägt in erster Linie der

Feinkornbeton die Zugspannungen, die Textilien tragen lediglich im Verhältnis ihrer relativ tiefen Steifigkeit bei. Mit Erreichen der Mörtelzugfestigkeit bildet sich ein erster Riss, gefolgt von einer zweiten Phase der Ausbildung vieler fein verteilter Risse. Nach Erreichen des abgeschlossenen Rissbilds wachsen in der dritten Phase die Rissöffnungen an bis zum Erreichen der Maximallast. Auch in dieser dritten Phase zeigt sich noch stets eine Verbundwirkung der Textilien mit dem Feinkornbeton (Zugversteifung, sogenanntes «tension stiffening»). Bei Erreichen der Maximallast eines textilbewehrten Zugkörpers können üblicherweise drei Versagensmechanismen beobachtet werden: Zugversagen aller Fasern im Garn (aufgrund der unvollständigen Tränkung mit Kunstharz jedoch für tiefere Spannungen als die Faserzugfestigkeit); Ausziehversagen der Fasern im Garnkern – üblicherweise bei der Garnverankerung –, bei dem der Garnmantel mit der Mörtelmatrix verbunden bleibt («sleeve effect», inneres Verbundversagen), auch als Schlupfversagen bezeichnet; und Ausziehversagen des ganzen Garns, beim dem Garnmantel und Garnkern ausgezogen werden (Verbundversagen am Interface zwischen Garn und Mörtelmatrix), evtl. mit vorgängiger Längsrissbildung und/oder Delamination zwischen Textilschicht und Feinkornbeton.

In der Biegeverstärkung bestehender Stalhbetonbauteile spielt daher die Vorbereitung des Untergrunds eine wesentliche Rolle. Zur Sicherstellung eines ausreichenden Verbunds zwischen der bestehenden Betonoberfläche und der Verstärkungsschicht aus Textilbeton muss der Untergrund mittels Hochdruckwasserstrahlen aufgeraut und vor Aufbringen des Feinkornbetons vorgenässt werden. Anschliessend wird eine erste, relativ dünne Schicht Feinkornbeton aufgebracht, üblicherweise im Spritzverfahren (trocken oder nass). Darauf folgen sukzessive Wechsel von Textilgitter und Feinkornbetonschichten (ca. 1 cm) bis zum Erreichen der geplanten Schichtstärke. Mit einer solchen Ausführungsmethode kann ein Verbundsagen an der Schnittstelle zwischen bestehender Betonoberfläche und Textilbeton i.d.R. vermieden werden.

Um geeignete theoretische Ansätze für die Bemessung der Biegeverstärkung vorwiegend einachsig tragender Stahlbetonplatten zu identifizieren, wurde eine Datenbank mit experimentellen Ergebnissen aus der Literatur erstellt. Diese Datensammlung enthält Resultate von etwa 150 Versuchen an verstärkten Versuchskörpern und unverstärkten Referenzkörpern, wobei jeder Datensatz jeweils 58 verschiedene Parameter abdeckt, wie Versuchsanordnung, Querschnittsgeometrie, Materialeigenschaften und experimentelle Bruchlasten. Der potenziell günstige Einfluss einer Biegeverstärkung mit Textilbeton auf den Querkraft- oder Ermüdungswiderstand sowie das Verhalten im Gebrauchszustand von Fahrbahnplatten konnte aufgrund nicht verfügbarer Literaturdaten hier nicht beurteilt werden.

Die meisten erfassten Versuche wurden mit Textilien aus Carbonfasern (33% aller Versuchsresultate) oder PBO-Fasern (45%) durchgeführt. Textilien mit Basaltfasern (14%) oder Glasfasern (8%) wurden wesentlich weniger häufig verwendet. Bei Verstärkungen mit Carbon wurde üblicherweise Delamination oder Ausziehversagen beobachtet. Bei PBO-Textilien wurde vorwiegend Delamination beobachtet, bei Basalttextilien zumeist Ausziehversagen. Glasfasertextilien konnten in der Hälfte aller Fälle zerrissen werden, die andere Hälfte der Versuchsresultate zeigte Delaminations- oder Ausziehversagen.

Die empirische Auswertung der Versuchsresultate zeigt, dass bei bis zu vier Textillagen – unabhängig vom Textilmaterial – jede Lage den Biegewiderstand, im Vergleich zum unverstärkten Referenzkörper, um etwa 20-25% erhöht. Bei 1-2 Textillagen wird üblicherweise Ausziehversagen beobachtet, während bei 3 Textillagen und mehr zumeist Delamination massgebend wird. Diese Auswertung wurde nicht weiter detailliert, z.B. bezüglich Einfluss von Textilmaterial oder -geometrie.

Die experimentellen Daten werden den Resultaten von verschiedenen theoretischen Ansätzen zur Berechnung des Biegewiderstands gegenüber gestellt. Ein erster Ansatz stellt auf den klassischen Annahmen für die Querschnittsanalyse von Stahlbeton ab (Ebenbleiben der Querschnitte, Vernachlässigung der Betonzugfestigkeit, Bewehrungen mit Kräften nur in Stabrichtung) und berücksichtigt starren Verbund zwischen Textil und Feinkornbeton. Die Resultierenden der Zug- und Druckkräfte im Querschnitt werden mittels Gleichgewicht, Ebenbleiben der Querschnitte (Dehnungsverträglichkeit) und üblicherweise verwendeter Materialgesetze bestimmt. Mit diesem Ansatz wird der experimentelle Biegewiderstand im Mittel um 18% überschätzt, bei einem Variationskoeffizienten (COV)

von 30% (unter Annahme einer Normalverteilung). In 80% der Fälle wird ein Biegewiderstand auf der unsicheren Seite berechnet. Der Ansatz wurde daher als ungenügend beurteilt. Aufgrund dieser Ergebnisse wird klar, dass Reduktionskoeffizienten auf die Axialsteifigkeit der Verstärkungstextilien eingeführt werden müssen, die aus den Besonderheiten des Verbunds im Textil selbst und des Verbunds vom Textil zum umgebenden Feinkornbeton entstehen. Mit den in der Fachliteratur postulierten Reduktionskoeffizienten wird die wirkliche Tragfähigkeit jedoch um fast 20% unterschätzt, wenn auch mit etwas reduziertem COV.

Der zweite untersuchte Ansatz geht deshalb ins andere Extrem, indem der Verbund zwischen Textil und Feinkornbeton bis auf die Verankerung vernachlässigt wird. Die Textilien werden als verbundfreie, endverankerte Bewehrungen betrachtet, ähnlich wie dies für Vorspannung ohne Verbund gemacht wird. Zur Bestimmung der mittleren Dehnung im Textil wird dabei ein Starrkörpermechanismus untersucht, dabei ist die berücksichtige freie Länge der Textilbewehrung zentral; hierfür wurde einerseits die theoretisch gerissene Länge im Textilbeton, und andererseits die Länge mit fliessender Stahlbewehrung berücksichtigt. Im ersten Fall werden die experimentellen Resultate im Mittel um 26% unterschätzt, mit einem COV von 24%. Nur 20% aller Fälle liegen auf der unsicheren Seite. Im zweiten Fall werden die experimentellen Resultate im Mittel um 12% unterschätzt, bei einem COV von 28%. Obwohl dieser Ansatz Resultate auf der sicheren Seite liefert, wurde die relativ hohe Variabilität als nicht zufriedenstellend erachtet.

Weitere Berechnungsansätze berücksichtigten Reibungs- resp. Verbundkoeffizienten (Dehnungslokalisierung), in Analogie zu Spanngliedern resp. Klebebewehrungen. Wegen der jeweils sehr hohen COV (> 50%) wurden auch diese Ansätze fallen gelassen.

Schliesslich wird ein analytisches Modell für die Bemessung im Grenzzustand der Tragsicherheit empfohlen, welches sich ebenfalls an Modellen von Klebebewehrungen orientiert, indem Dehnungsbegrenzungen für die Biegeverstärkung mit Textilbeton bei gleichzeitigem Fliessen der bestehenden Stahlbewehrung eingeführt werden. Die Dehnungsbegrenzungen in den Textilien werden anhand der experimentellen Resultate so kalibriert, dass diese im Mittel genau abgebildet werden. Die Beurteilung der Resultate erfolgt anhand der zugehörigen COV. Unabhängig von Textilmaterial und Versagensart ergibt sich für die Dehnungsbegrenzung ein Mittelwert von 6.6‰ und ein COV von knapp 17%. In einem weiteren Schritt werden Mittelwerte der Dehnungsbegrenzungen nach Textilmaterial unterschieden (Carbon: 4.5‰, PBO: 8‰, Basalt: 12‰, Glas: 8‰), womit der COV unter 16% gesenkt werden kann. Mit einer weiteren Unterscheidung der Mittelwerte der Dehnungsbegrenzungen pro Textilmaterial je nach experimentell beobachteter Versagensart lassen sich die COV noch weiter reduzieren (Carbon: 14%, PBO: 12%, Basalt: 16%, Glas: 9%). Diese werden als ausreichend tief bewertet, angesichts der im Betonbau üblicherweise anzutreffenden Variabilität.

In der praktischen Bemessung der Textilbetonverstärkung dürfen im Biegenachweis selbstverständlich keine Mittelwerte, sondern müssen Bemessungswerte der Dehnungsgrenzen berücksichtigt werden. Diese stellen wiederum auf charakteristischen Werten ab und berücksichtigen weitere partielle Sicherheitsfaktoren und Umrechnungskoeffizienten. Für Carbon- und PBO-Textilien können charakteristische Werte aus den kalibrierten Mittelwerten der Dehnungsbegrenzungen und den COV unter der Berücksichtigung der Anzahl verfügbarer Versuchsresultate abgeleitet werden zu 4.2‰ für Carbon und 6.9‰ für PBO. Für Basalt- und Glasfaserbasierte Textilien standen zu wenig Resultate zur Verfügung, um charakteristische Werte abzuleiten. Die Festlegung von partiellen Sicherheitsfaktoren und Umrechnungskoeffizienten, erforderlich in der Berechnung von Bemessungswerten, bedarf hingegen weiterer Untersuchungen, insbesondere für PBO-Textilien. In der Literatur finden sich lediglich Angaben für Carbon- und Glasfasertextilien, die einen Materialsicherheitsfaktor von 1.3 und Umrechnungskoeffizienten von 0.85 (Carbon) resp. ca. 0.4 (Glas) empfehlen.

Dieses Bemessungsvorgehen hat den Vorteil, dass es praxisorientiert ist, indem es auf gängigen Praktiken abstellt. Der Nachteil ist, dass die massgebende Versagensart nicht direkt abgebildet wird, sondern auf eine Dehnungsbegrenzung (resp. ein «künstliches» Faserversagen) im Querschnitt der maximalen Biegebeanspruchung reduziert wird. Dies, obwohl in Versuchen eher Ausziehen oder Delamination beobachtet werden. Bei

Ausziehen versagt die Verankerung der Textilien, während bei Delamination der Verbund an der Schnittstelle von erster Textilschicht und umgebendem Feinkornbeton versagt. Beide Versagensarten finden sich in Bereichen mit hoher Schubbeanspruchung resp. in Auflagernähe.

Die vorgeschlagene Biegebemessung mittels Dehnungsbegrenzung soll daher mit einem Nachweis der Verankerung des Textils im theoretisch ungerissenen Bereich (hinter dem ersten Riss, analog zu SIA 166 für Klebebewehrungen) ergänzt werden. Damit sollte eine ausreichend konservative Bemessung möglich sein. Der vorliegende Bericht führt ebenfalls ein Modell zum Nachweis dieser Verankerung von Textilien im Feinkornbeton ein. Dieses stellt auf einem theoretischen Modell aus der Literatur für das Verbundverhalten eines einzelnen Faserstrangs ab sowie auf eigenen Versuchsresultaten und solcher aus der Literatur für ganze Textilien. Das vorgeschlagene Bemessungsmodell für die Verankerung zeigt eine gute Übereinstimmung mit den Versuchsresultaten sowie zufriedenstellende Variationskoeffizienten. Ausserdem zeigt dieses Modell auch, dass die verankerbare Textilspannung bei Vergrösserung der Verankerungslänge nicht beliebig erhöht werden kann, da die Verbundbruchenergie beschränkt ist, und dass der Zugwiderstand des Textils in der Regel nicht ausgeschöpft wird.

Die Anwendung von Textilbeton zur Biegeverstärkung von Stahlbetonplatten ist eine praxistaugliche und brauchbare Alternative zu Klebebewehrungen aus faserverstärkten Kunststoffen. Die grössten Vorteile von Textilbeton bestehen in der einfachen Anwendung vor Ort, die mit auf der Baustelle gut eingeführten Methoden arbeitet, im klar besseren Brandwiderstand sowie in der vergrösserten Betonüberdeckung für die bestehende Stahlbewehrung.

Künftige Untersuchungen zur Anwendung von Textilbeton als Verstärkungsmethode von Stahlbeton sollten den Einfluss des Verbunds zwischen Textil und Feinkornbeton auf das Tragverhalten von Fahrbahnplatten in der Verstärkungszone in den Grenzzuständen der Gebrauchstauglichkeit und der Tragsicherheit sowie den potentiell günstigen Einfluss einer solchen Biegeverstärkung auf deren Querkraftwiderstand umfassen. Dabei sind insbesondere grossmassstäbliche Versuche mit Verstärkungen aus Basalt- und PBO-Textilien zur Validierung des Dehnungsbegrenzungsansatzes sowie seine Erweiterung auf generellere Situationen (hohe Stahlbewehrungsgrade in der bestehenden Betonplatte, grössere Variabilität der Plattenschlankheit etc.) wünschenswert, ebenso die Identifikation massgebender Querschnitte für die Bemessung.

Der Einfluss der Biegeverstärkung aus Textilbeton auf die Ermüdungsfestigkeit einer bestehenden Fahrbahnplatte aus Stahlbeton sowie die mögliche Reduktion der Verstärkungswirkung des Textilbetons infolge Ermüdungslasten sind weitere wichtige zu untersuchende Themen. Ferner sollte auch die Effizienz von mehreren Textillagen, insbesondere drei und mehr, untersucht werden. Dazu werden Verankerungsversuche mit variabler Länge sowie grossmassstäbliche Biegeversuche empfohlen, in denen auch die Beanspruchungsseite mit den üblicherweise massgebenden Achslasten wirklichkeitsnah abgebildet werden. Die Resultate sollten hinsichtlich Effizienzfaktoren der reinen Textilien in Zusammenhang mit dem Verbundverhalten evaluiert werden. Mit ergänzenden theoretischen Untersuchungen kann damit die Zugversteifungswirkung von Textilbeton über den gesamten Verstärkungsbereich von Fahrbahnplattenstreifen aus Stahlbeton beschrieben werden. Dazu kann das in diesem Bericht beschriebene Verbundmodell als Ausgangslage dienen.

Diese Untersuchungsresultate sollten sich nicht zuletzt in normativen Richtlinien (national anwendbar, z.B. mittels Revision der bereits 15-jährigen SIA 166) niederschlagen, die zudem die Ermittlung von charakteristischen Kennwerten, Umrechnungs- und partiellen Sicherheitsfaktoren auf der Materialseite erfordern.

Résumé

Ce rapport présente les résultats de l'évaluation de l'aptitude de différentes approches analytique pour le dimensionnement à l'état-limite ultime (ELU) d'un renforcement à la flexion des dalles de roulement des ponts-routiers avec du béton armé aux textiles (béton textile, BT).

Le BT est un matériau composite qui combine la résistance à la traction élevée des fibres des textiles avec l'adhérence et les protections mécaniques et thermiques fournies par des bétons à petits granulats, c.à.d. des mortiers à base de ciment. En plus d'être utilisé dans la fabrication de nouveaux éléments en BT, ce matériau peut également être utilisé en tant que couches de renforcement d'éléments en béton armé (BA) existants. Les textiles les plus populaires utilisées dans ce type d'application se composent de fibres de carbone, de basalte, de verre et de PBO (polyphénylène-2,6-benzobisoxazole, alias « Zylon »). Après leur production, ces fibres sont regroupées en fils très résistants à l'aide de résine. Ces fils sont ensuite tissés en textiles, normalement en forme de grilles.

Pour le renforcement à la flexion d'éléments BA existants, la préparation du support joue un rôle crucial. Afin d'assurer un comportement monolithique à l'interface, il doit être rendu rugueux par l'hydrodémolition avant d'appliquer le système de renforcement. Une fois ce processus terminé, la première couche de mortier peut être appliquée, normalement par giclement à voie sèche ou humide, suivie par des couches successives de textile-mortier jusqu'à ce que le niveau de renforcement souhaité soit atteint.

En plus d'offrir un enrobage supplémentaire à l'armature en acier dans un élément BA existant, le mortier joue un rôle structural important pour l'ancrage des textiles au bord de la zone fonctionnelle. L'ancrage par adhérence a été étudié à travers d'une campagne expérimentale qui a permis de compléter des données expérimentales de la littérature et de calibrer une série de paramètres d'un modèle théorique précédemment développé. L'étude s'est conclue par la proposition d'une approche analytique pour le calcul de la résistance d'ancrage des fils des textiles noyés dans le mortier. Des détails concernant cette proposition et l'étude expérimentale figurent aussi dans le présent rapport.

Afin d'identifier une approche théorique appropriée pour le dimensionnement du BT en tant que renforcement à la flexion des dalles unidirectionnelles, une base de données de résultats expérimentaux a été créée en rassemblant des données de la littérature existante. Elle contient les résultats d'environ 150 expériences sur des éléments renforcés et non renforcés de référence. Chaque entrée couvre 58 paramètres relatifs à la configuration de test, la géométrie des sections, les propriétés des matériaux et les résultats expérimentaux.

Dans un premier temps, ces données ont été évaluées empiriquement pour déterminer statistiquement le type de matériel de textile utilisé, les types de défaillances observés et l'augmentation de la résistance à la flexion. Cette dernière est augmentée, à la moyenne et indépendamment du matériau de textile, de 20-25% par couche de textile. Différentes approches analytiques ont été ensuite appliquées afin de tester leur adéquation, en comparant la résistance à la flexion théorique avec les résultats expérimentaux.

Une première approche considère l'adhérence du textile à la matrice comme rigide et a pour résultat une forte surestimation de la résistance réelle à la flexion avec un grand coefficient de variation (COV) encore. Ce que justifie l'introduction des coefficients de réduction de la rigidité axiale des textiles, comme aussi postulé dans la littérature, qui résident dans les particularités du comportement à l'adhérence à l'interne des textiles mais aussi avec le mortier qui les enrobe.

La seconde approche appliquée va donc vers l'autre extrême, en considérant qu'il n'y a pas d'adhérence entre le textile et la matrice mais que le textile est ancré à l'extrémité de l'élément par le mortier. Cette approche donne des résultats conservateurs de la résistance théorique à la flexion mais n'est pas non plus considérée comme satisfaisante, en raison du COV élevé. Les troisième et quatrième approches appliquées cherchent à identifier des coefficients de frottement respectivement des coefficients d'adhérence entre le textile et la matrice mais, en raison de leur inapplicabilité pour les configurations de flexion 3 points et des COV élevés, ces approches ont aussi été abandonnées.

Enfin, une méthode analytique est retenue, qui introduit des déformations-limites à la traction par flexion pour les textiles pendant que l'armature en acier existante est en écoulement, en s'orientant ainsi à des approches provenant des lamelles en polymère renforcées par fibres collées. Grâce à la calibration raffinée de ces limites, une moyenne de 1 du rapport entre les résultats expérimentaux et théoriques et le COV le plus bas de toutes les approches évaluées sont obtenus.

Cette approche a l'avantage d'être bien orienté vers la pratique. Le désavantage est que le mode de rupture prépondérant ainsi n'est pas explicitement décrit par cette vérification. Dans les essais, on observe normalement des ruptures de l'ancrage ou de délamination des textiles qui sont plutôt liés, les deux, à une sollicitation à l'effort tranchant qu'à la flexion. Ainsi, il est recommandé de compléter le dimensionnement à la flexion par déformations-limites avec la vérification de l'ancrage des textiles dans la zone théoriquement non-fissurée (en analogie avec la SIA 166). Ce rapport présente aussi un modèle de dimensionnement pour la vérification de l'ancrage des textiles qui montre une bonne concordance avec des résultats expérimentaux et des COV satisfaisants. En plus, il démontre que la résistance de l'ancrage est limitée et que la résistance à la traction des textiles ne peut normalement pas être exploitée.

Pour le dimensionnement pratique avec les déformations-limites, il y a besoin d'identifier des valeurs de dimensionnement qui se basent, à leur tour, sur des valeurs caractéristiques. Des déformations-limites pour ces derniers ne peuvent pratiquement être recommandées qu'uniquement pour les textiles en fibre de carbone ou de PBO car trop peu de données étaient disponibles pour les textiles en fibre de verre et de basalte.

Le béton armé aux textiles ou le béton textile représente une méthode viable pour renforcer les éléments structuraux existants en béton armé à la flexion. Les avantages principaux de cette méthode de renforcement sont la facilité d'application sur le chantier, qui implique des outils déjà utilisés, ainsi qu'une meilleure résistance au feu en comparaison avec des solutions utilisant des armatures collées.

L'incidence potentielle du renforcement à la flexion avec du béton textile sur la résistance au cisaillement ou à la fatigue ainsi que sur le comportement à l'état de service des dalles de roulement n'a pas pu être évalué en raison de l'indisponibilité de données dans la littérature. Des recherches sur cet effet sont clairement souhaitable, portant, en particulier, sur des essais en grandeur réaliste avec des renforcements aux textiles en basalte et en PBO et sur des situations plus générales (taux d'armature en acier plus élevés, autres élancements des dalles etc.). Ainsi, des déformations-limites pour ces matériaux peuvent être établies et des sections de contrôle peuvent être identifiées plus précisément.

Les effets des renforcement textile seront bien probablement affectés par l'influence de l'adhérence entre textile et mortier sur le comportement de l'élément renforcé où des recherches supplémentaires devraient aussi être effectuées. Une attention particulière devrait être prêtée à l'évaluation de l'efficience de trois couches de textiles et plus, à identifier par des essais d'ancrage à longueur variable et par des essais à la flexion en grandeur réaliste. Ces résultats, en combinaison avec des réflexions théoriques ultérieures devraient permettre de décrire le comportement des textiles et leur adhérence. Une perte potentielle de la capacité du renforcement en béton textile due à la sollicitation par des charges de fatigue serait un autre sujet important à étudier. Pour ces deux sujets, le modèle d'adhérence décrit dans ce rapport peut servir comme base.

Enfin, les résultats de toutes ces évaluations devraient de refléter dans des directives normatives (p.ex. par une révision de la SIA 166). Ceci nécessitera, en plus, la dérivation et l'identification des valeurs caractéristiques, des coefficients de conversion et des facteurs des sécurité des matériaux.

Summary

This report presents the suitability evaluation of various theoretical approaches for the structural design of the flexural strengthening of bridge deck slabs with textile reinforced concrete (TRC) at ultimate limit state (ULS).

TRC is a composite material which combines the high tensile strengths of the fiber textiles with the bond capacity and the mechanical and thermal protection provided by fine-grained concrete (i.e. cement-based mortars). Besides being used in manufacturing of new TRC elements, these materials can also be used as strengthening for existing reinforced concrete (RC) elements. The most frequently used textiles in this type of applications are made from Carbon, Basalt, Glass and PBO (poly-phenylene-2,6-benzobisoxazole a.k.a. Zylon) fibers. Such fibers are bundled together into highly resistant yarns with the help of resin. These yarns are then woven into textiles, usually applied in the form of meshes.

In flexural strengthening of existing RC elements, the preparation of the support surface plays an important role. It has to be roughened by hydro-demolition before applying the strengthening system in order to ensure a monolithic behavior at the interface. Once this process is completed, the first mortar layer can be applied, usually by spraying, followed by successive textile-mortar layers until the desired strengthening level is reached.

Besides offering a protection layer to the steel reinforcement of the existing RC element, the mortar plays an important structural role as anchorage and bond agent for the textile yarns. The anchorage by bond was studied in an experimental campaign, complementing existing experimental data from the literature and allowing to calibrate a series of parameters of the theoretical model proposed in the literature. The study concluded with an analytical proposal for determining the bond anchorage capacity of the textile yarns embedded in mortar. More details on the proposal and the experimental campaign are given in this report.

To identify a suitable theoretical approach for dimensioning the flexural strengthening of existing one-way slab elements, a database with experimental results was created by gathering data from the literature. This database contains data from approximatively 150 experiments on strengthened elements and unstrengthened reference elements. Each entry describes 58 different parameters covering input data such as test setup, cross-sectional geometry, material properties and experimental failure loads.

In a first step, the collected data was evaluated empirically to statistically determine the type of textile materials used, the types of observed failure and increases in flexural capacity. The latter increases, on average and independently of the textile material, by 20-25% per textile layer. In a second step, different theoretical approaches for ULS design of the flexural strengthening of slab elements with TRC were applied to evaluate their suitability by comparing the theoretical flexural capacity with the experimental results.

A first approach considers rigid bond between textile and surrounding concrete matrix and results in a large overestimation of the flexural capacity and a high coefficient of variation (COV). This legitimates the introduction of efficiency coefficients on the axial stiffness of the textiles, as also proposed in literature, which are due to the particularities of internal bond of the textiles but also to the bond between textile yarns and the surrounding mortar.

Thus, the second approach applied goes into the other extreme, considering no bond between textile and matrix but end-anchorages of the textile being provided by the mortar. This approach returns conservative estimations of the flexural capacity, yet it is not satisfactory due to a high COV. The third and fourth approaches applied evaluate the consideration of friction and bond coefficients, respectively, between textile and surrounding matrix. However, due to their inapplicability to 3-point bending configurations and high COVs, they were also considered unsatisfactory.

Finally, an analytical method is retained that introduces strain limits for the flexural tension forces in the textiles while the existing steel reinforcement is yielding, thereby relating to approaches known from fiber-reinforced polymer strips. Thanks to thoughtful calibration of the strain limits, this approach results in an average of 1 for the ratio between experimental results and theoretical predictions and the lowest COV of all evaluated approaches.

This approach has the advantage of being aptly practice-oriented. However, such a dimensioning approach does not explicitly address the governing rupture mode. In load tests, anchorage or delamination failures of the textiles are normally observed which are, both, rather related to loading from shear forces than bending moments. As such, it is recommended to complement the flexural dimensioning by strain limits with a verification of the anchorage capacity of the textiles in the theoretically uncracked zone (in analogy to SIA 166). This report also presents a dimensioning model for this anchorage capacity that shows good agreement with experimental results and acceptable COV. Furthermore, the model also proofs that the anchorage capacity is limited and that the tensile strength of the textiles can usually not be exploited.

For a practical dimensioning, design values of the stain limits are required, being based on characteristic values. Practically applicable strain limits for the latter can be recommended for carbon and PBO fiber textiles only, as too few experimental data is available for textiles made of glass and basalt fibers.

Textile reinforced concrete represents a viable method for strengthening existing reinforced concrete elements in bending. The main advantages of this strengthening method are the ease of application which involves tools that are already in use on the construction site, and better fire resistance compared to adhesively bonded solutions with fiber-reinforced polymers.

The potential impact of flexural strengthening with TRC on shear or fatigue capacity as well as the serviceability behavior of deck slabs could not be assessed due to missing literature data. Further investigations are required on the influence of bond between textile and matrix on the strengthened length, and to determine the effects of flexural strengthening with TRC on the shear strength of bridge deck slabs. A potential strengthening capacity loss over time due to fatigue loading is a further important subject to be studied.

Such investigations should target real-scale tests with basalt and PBO strengthening and, in addition, more general structural conditions (higher steel reinforcement ratios, more variable slab slenderness etc.). Particular attention should be given to the identification of the efficiency of three and more textile layers, to be identified in anchorage tests with variable anchorage length and real-scale flexural tests. In combination with additional theoretical evaluations on the influence of the textile bond behavior over the whole strengthened length, such results would allow to refine the proposed strain limits and to identify governing control sections in more detail. The textile bond model presented here can serve as a basis for all these investigations.

Last but not least, the results and conclusions of such evaluations should be reflected in normative guidelines (e.g. through a revision of SIA 166). This will further require the derivation and identification of characteristic values, conversion coefficients, and partial safety factors for the strengthening materials.

1 Introduction

Applications of textile reinforced concrete are gaining attention since a couple of decades. Today, they are used in various types of prefabricated elements where high strength and reduced self-weight are required, or where steel reinforcement cannot be used due to potential corrosion issues. However, their application as a strengthening method becomes more and more a point of interest.

The research presented in this report was conducted to identify appropriate theoretical approaches for dimensioning textile reinforced mortar layers (also known as textile reinforced concrete TRC or fabric reinforced cementitious matrix FRCM) to strengthen bridge deck slabs in bending. Various analytical approaches are compared to experimental data from the literature to assess their suitability.

This study focusses on flexural strengthening of reinforced concrete slabs at the ultimate limit state (ULS) only. The effect of TRC strengthening on shear and fatigue capacity as well as on improvements of the structural behavior in the serviceability limit state (SLS) of slab elements was not investigated due to the lack of experimental studies in the literature of these particular aspects.

2 Basic materials

2.1 Textile reinforcement

Technical fabrics made of artificial fibers were first used as a concrete reinforcement alternative at the Sächsisches Textilforschungsinstitut in Germany at the beginning of the 1980's [1]. The first textile reinforced concrete element was used for road safety barriers where, for durability reasons, steel reinforcement should be avoided.

2.1.1 General description and production process of reinforcement textiles

The fibers composing the yarns of technical fabrics or textiles, respectively, are made of materials with high tensile strength and relatively high elastic modulus. These fibers are usually produced by extrusion from various materials, such as glass and basalt or from polymers characterized by long molecule strings like poly-phenylene-2,6-benzobisoxazole PBO (also known as "Zylon"), aramid, polyamide or polypropylene. Carbon fibers are made from other organic polymer fibers which go through a high temperature, oxygen-less process called carbonization [2].

The fibers are later combined into strings which can be twisted into yarns or woven into fabrics. The length of these fibers can reach hundreds of meters, having practically no production length limit. The linear mass density of a fiber is measured in *tex* (g/km) and it can vary from less than 1 *tex* to more than 100 *tex* as a function of the material.

For reinforcing concrete, the woven textile yarns could not be used unless adhesively bonded. Therefore, textile grids were developed to be integrated within a mortar matrix. The textile mesh is habitually made of yarns equally spaced and orthogonally woven (Figure 1). Usually, these meshes are designated as bidirectional (warp and weft) or unidirectional (warp only) in view of significant load-bearing capacity in the respective fabric directions.

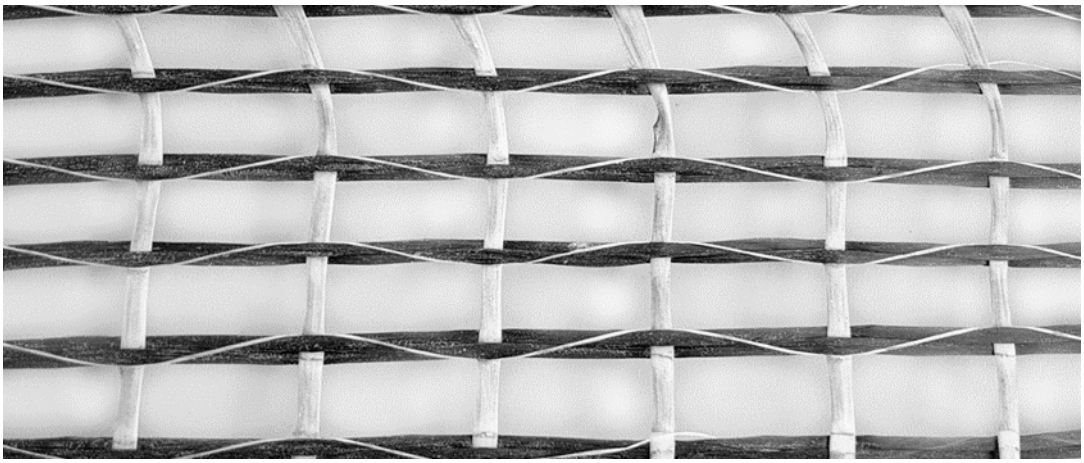

Figure 1 *Unidirectional textile mesh (black carbon fiber yarns in warp direction and white glass fiber yarns in weft direction).*

2.1.2 Usual geometries of yarn and mesh

The yarn spacing usually varies between 10 to 40 mm, but can also be as low as 5 mm. The yarn normally has an elliptical shape with *D/d* ratio from 1 (circle) to 10 (very flat ellipse), Figure 2, varying from one fabric provider to another, while its cross-section is also highly variable, from as low as 0.2 mm^2 up to 3 mm^2. The shape of the cross-section or the *D/d* ratio, respectively, has a high impact on the bond capacity of the yarn to the cementitious matrix [3]. Generally, the larger is the perimeter of the yarn, the higher is its bond capacity.

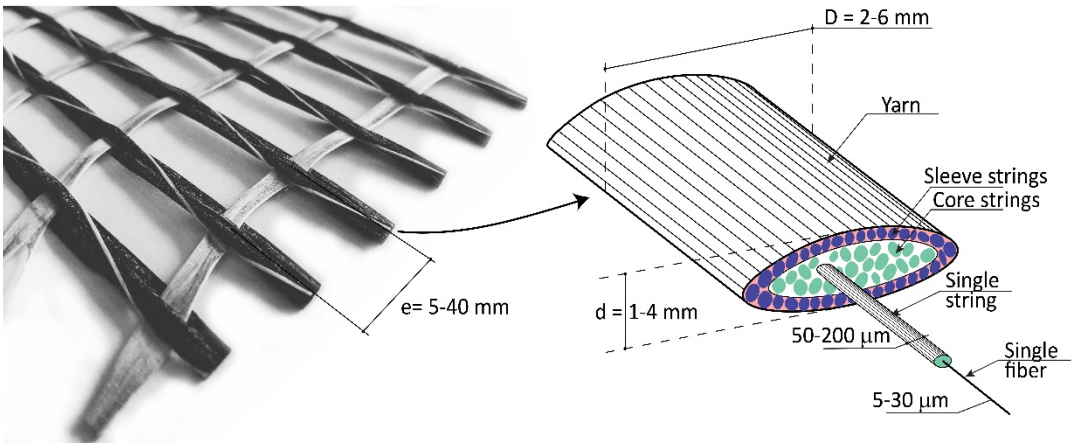

Figure 2 *Mesh and yarn geometry (inspired from [4])*

2.1.3 Mechanical properties and behavior of fibers

The most popular technical textiles for TRC are made of carbon [5], PBO [6], basalt [7], and glass fibers. Their mechanical behavior is quasi-brittle, that is, approximately linear elastic up to tensile failure.

PBO fibers have the highest tensile strength (5'800-6'000 MPa) and the highest elastic modulus (270-280 GPa). Carbon fibers have slightly smaller mechanical properties while basalt and glass fibers have considerably lower strength and elastic modulus (Table 1).

Table 1 *Mechanical properties of usual yarn materials*

Material	E_f	$f_{f.u}$	$\varepsilon_{f.u}$
	[GPa]	[MPa]	[‰]
Carbon	240	4'300	17.9
PBO	280	6'000	21.4
Basalt	90	3'000	33.3
Glass	80	2'600	32.5

These mechanical properties do not change significantly over time, i.e. the fibers are very durable [8]. For glass fibers, there used to be an issue with alkali resistance but thanks to the development of new fiber types (alkali-resistant glass, AR-glass), this durability problem could be resolved since.

The only remaining major durability issues for textile fibers, especially for polymer drawn fibers, are temperatures above approx. 300°C which can lead to carbon oxidation (i.e. transforming carbon into CO2). Covering the textile reinforcement by already small mortar layers usually increases the fire resistance to a satisfactory level [9], thereby offering an important advantage over externally bonded reinforcement. 300°C is attained in a textile with 2 cm mortar cover after approx. 60' of exposure to the Unity Temperature Curve ('Einheits-Temperatur-Kurve', DIN 4102-2 1977) [9].

Figure 3 shows constitutive laws for typically applied fiber materials, for single fibers and yarn, in comparison to a bilinear simplification for regular reinforcing steel (average values). In structural design situations, the high tensile strengths of the fibers cannot be exploited. When textile fibers are bundled to yarns, they are glued together by resin. This resin has different mechanical properties than the fibers which leads to a variable activation of the fibers in tension and so, to a different mechanical behavior of yarns in comparison to the basic fiber. It can also be that, during the fabrication process, the resin does not completely penetrate the yarn and empty spaces are formed between the fibers.

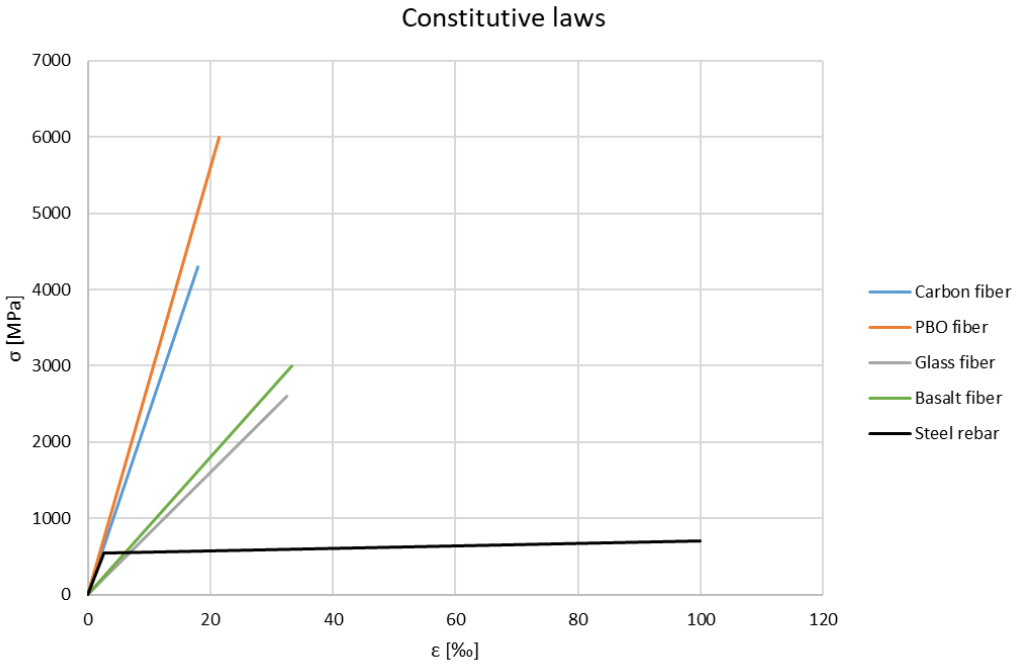

Figure 3 *Constitutive laws for carbon, PBO, basalt and glass fibers in comparison to regular reinforcing steel (B500B)*

Given these fabrication factors, together with the yarn shape which additionally allows sleeve effects to occur (Figure 2), an efficiency coefficient η needs to be introduced to describe the constitutive law of textile yarns. It accounts for all the imperfections as a reduction factor applied to the ultimate tensile strength of the fibers. Given their elastic behavior, this efficiency coefficient can be equivalently applied to the ultimate strain or the gross cross-section area of a yarn, respectively; that is, it results in a horizontal or vertical cut-off of the constitutive laws shown in Figure 3. Recommended values for this efficiency coefficient η are shown in Table 2 [10].

Table 2 *Efficiency coefficients η for textile yarns*

Fibers for textile yarns	η
Carbon	0.20
PBO	0.25
Basalt	0.25
Glass	0.25

The efficiency factors in Table 2 refer to textile yarns bonded in a mortar matrix. However, if tension tests on textile yarns are performed, sleeve effects are observed as well, and the tensile strength of the single fiber cannot be exploited, either. As an example, results from tension tests on a single yarn alone [9] show that the efficiency factor referring to the tensile strength of the fibers alone results in approx. 0.67. Hence, the tensile strength of the fibers cannot be exploited in any case, unless the production processes of yarns are improved such that they are completely saturated with an infinitely stiff polymer matrix, allowing rupture of all fibers. But, also in this case, the ultimate stress of a yarn will never attain the tensile strength of the fiber as there will always be a ratio of fibers to gross cross-section lower than one.

2.2 Mortar matrix

The mortar or cementitious matrix, respectively, is produced as wet mixture of fine-grained sand and cement that can be applied manually on the support (i.e. surface receiving the strengthening) or by using compressed air to spray it through a nozzle. The mortars used for TRC are part of a complete system, that is, manufacturers usually provide strengthening textiles and mortars at the same time.

Support preparation according to manufacturer prescriptions is necessary to ensure that failure will not occur at the interface of mortar to concrete. In strengthening of concrete elements, the mortar is applied after the support was roughened through hydro-demolition, cleaned and wetted (to avoid capillary suction of the water contained in the sprayed mortar). In other words, this preparation allows to actively avoid a potential failure at the interface between strengthening layer and support.

2.2.1 Mechanical properties and behavior

The mechanical properties and behavior of the mortars are similar to normal performance concrete. The compressive strength varies between 15 MPa and 60 MPa while the elastic modulus is between 10 GPa and 40 GPa. The (flexural) tensile strength of the mortar can be as high as 15% of the compressive strength. If not available and experimental testing is not an option, the average tensile strength (f_{ctm} [MPa]) can be computed as a fraction of the characteristic compressive strength (f_{ck} [MPa]), as in Eq. (2.1). Similarly, the elastic modulus (E_{cm} [GPa]) can also be computed from the average compressive strength (f_{cm} [MPa]), Eq. (2.2) [11].

$$f_{ctm} \approx 0.3 f_{ck}^{2/3} \tag{2.1}$$

$$\mathrm{E_{cm}} \approx 22 \left(\frac{\mathrm{f_{cm}}}{10}\right)^{0.3} \tag{2.2}$$

2.2.2 Long-term behavior

Mortars, similarly to concrete, have a good long-term behavior with some increase of the compressive strength over time. The main external damaging factor is frost, especially in moist environments. In these cases, the use of water-resistant mortars or other water-repellent measures are recommended. Since there is no steel reinforcement (which might be prone to corrosion) in TRC and other chemical attacks are unlikely to happen on the bottom face of bridge deck slabs, no particular measures nor important mortar cover thicknesses are needed for the strengthening textiles.

Some attention may possibly be needed for alkali-silica reaction (ASR) resistance of the applied mortars, in particular to the silica content of added aggregates (usually quartz sand).

3 Mechanical behavior of textile reinforced concrete

Embedding textile grids in cementitious matrices results in high performance composite materials which present important advantages in comparison to externally bonded reinforcement, given the high tensile capacity of the textile and the protective properties of the mortar.

Their composite behavior is usually studied in uniaxial tension. Tests are done according to RILEM recommendations [12]. Specimens (also known as RILEM planks) have the dimensions and are tested in a setup as shown in Figure 4.

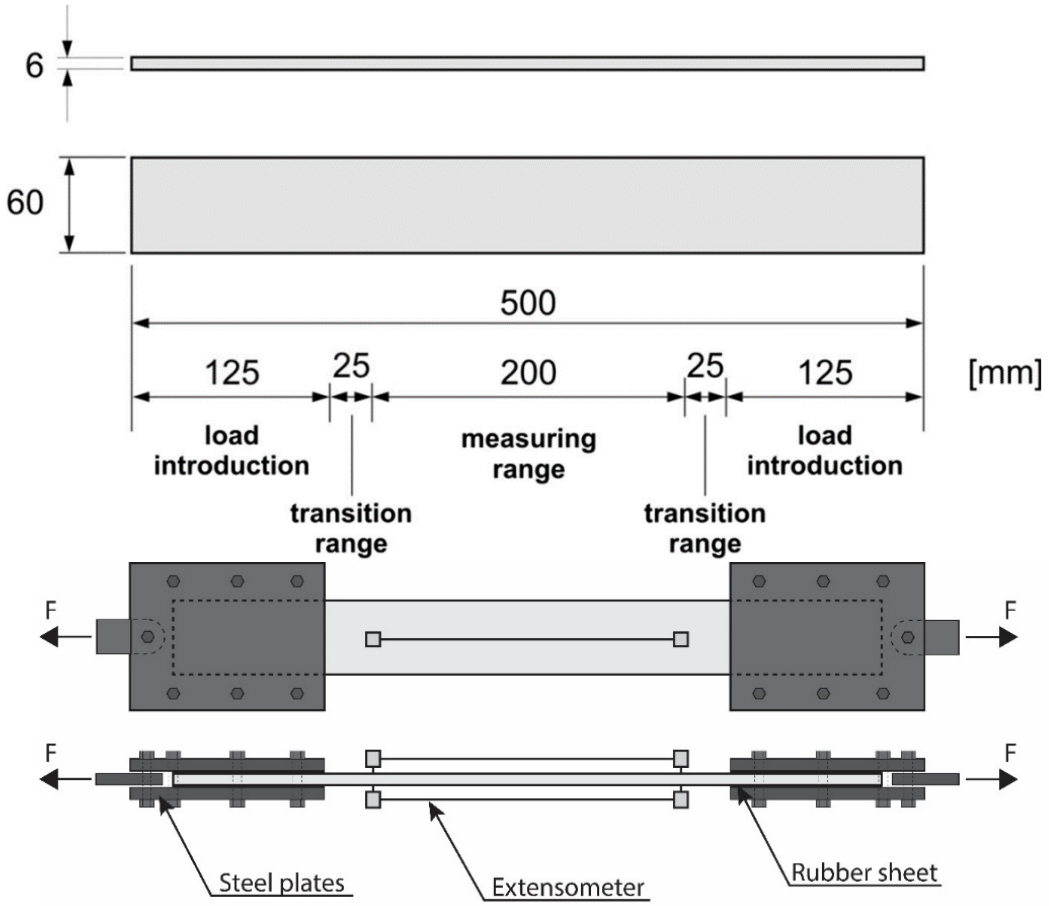

Figure 4 *TRC specimen geometry and test set-up requirements according to RILEM [12]*

3.1 Experimental observations

The stress-strain behavior of TRC as a composite material is multilinear with three distinct stages (Figure 5).

The first stage is an uncracked, linear elastic stage ① where the tensile force primarily passes through the mortar while the textile only provides a small contribution to load bearing, according to stiffness ratios. At reaching the mortar's tensile strength, the first crack forms ②, followed by the second stage of crack formation with the development of multiple cracks ③. The third stage starts after the crack pattern has fully developed, characterized by increasing crack openings ④ until failure of the composite material ⑤ is reached.

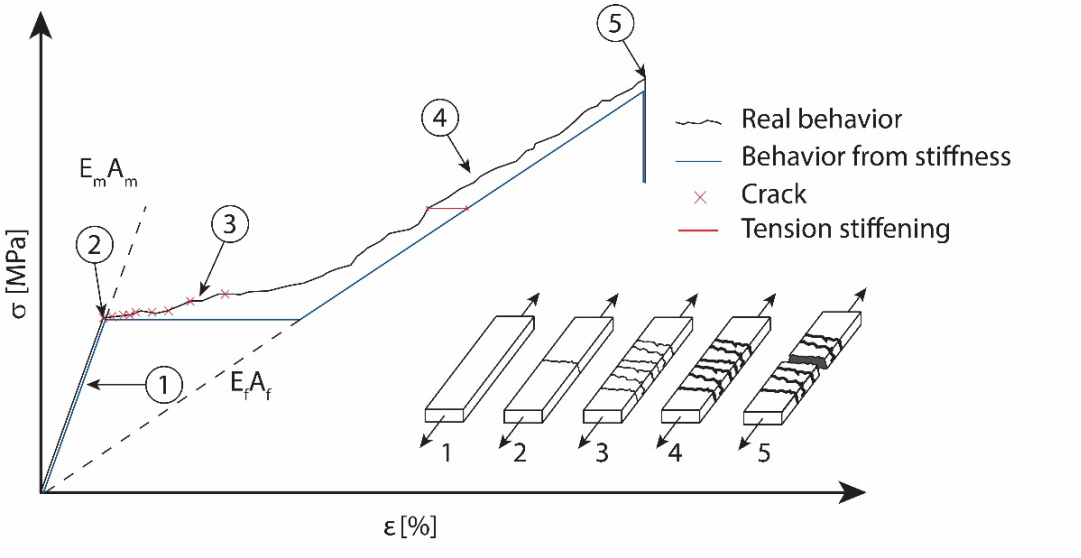

Figure 5 *Tensile behavior of TRC (inspired from [4])*

When comparing the experimental with a theoretical behavior which considers the stiffness of the mortar in the first stage only and the stiffness of the textile reinforcement in the third stage only, it can be observed that a tension stiffening effect is present in this latter stage. This implies that there is some bond between the textile and the mortar until failure. There are three potential failure mechanisms [13]:

- Rupture of the textile fibers – sleeve and core filaments (see Figure 2) all fail in tension
- Pull-out failure of the core filaments, usually in the anchorage zone of the textile – the sleeve filaments remain bonded to the mortar matrix while the core filaments are pulled-out (failure due to inner debonding in the yarn)
- Pull-out failure of the complete yarn – sleeve and core filaments are pulled-out as a whole (failure due to debonding at the yarn-mortar interface, possibly preceded by longitudinal splitting or delamination, respectively)

3.2 Bond capacity

Bond behavior of reinforcing elements in or externally bonded to concrete generally is described by bond stress-slip relationships.

Several bond stress-slip models to compute the pull-out strength of a single textile yarn embedded in a mortar matrix or externally bonded reinforcement (EBR), respectively, can be found in literature.

The parametric study done by Maeder [14] shows that the models from Mobasher [15] and Ulaga [16] are the most appropriate ones to model the bond behavior of a textile yarn. These two models are similar: the main difference is the assumption considered for the descending branch of the bond stress-slip relation. Ulaga – who developed his bond model for externally bonded fiber-reinforced polymer (FRP) lamellas – assumes a linearly descending behavior after reaching the maximum bond stress (Figure 6) while Mobasher – who developed his model for embedded FRP yarns, i.e. TRC – considers a stepped descending behavior (Figure 8).

A third model for TRC, proposed by Richter [17], considers a similar behavior as the one proposed by Ulaga, yet at the end of the unloading branch a constant bond stress is added (Figure 7), similarly to what Mobasher proposes (see 3.2.1).

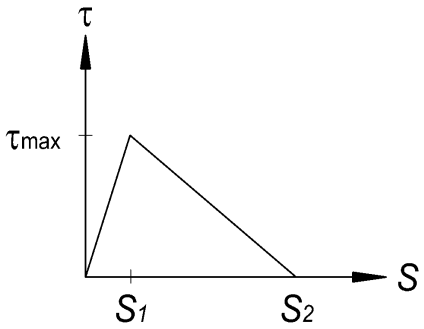

Figure 6 *Bond stress-slip relationship proposed for EBR by Ulaga [16]*

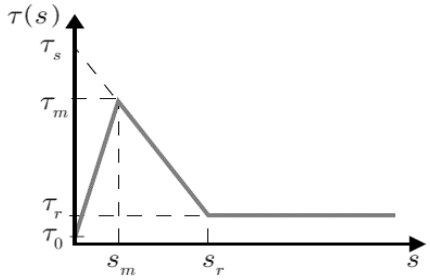

Figure 7 *Bond stress-slip relationship proposed for TRC by Richter [17]*

3.2.1 Bond behavior of a single yarn – Mobasher's model

The parameters of Mobasher's bond stress-slip model [15] can be calibrated from pull-out tests on textile reinforced concrete (TRC).

The bond stress-slip behavior is divided into three stages: a first stage with linearly increasing bond stress, followed by a stage with constant bond stress where partial debonding of the yarn results in a non-linear pull-out behavior, and a third stage with a rigid body motion of the yarn being pulled-out (stages I, II and III in Figure 8, respectively).

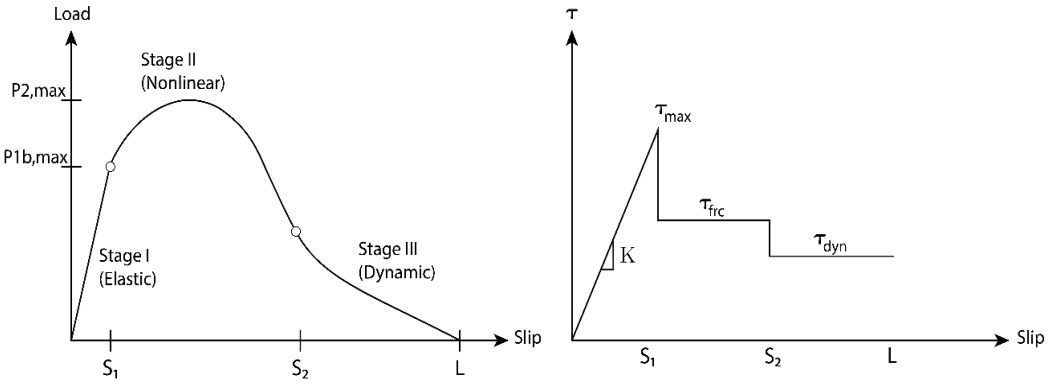

Figure 8 *Global load-slip response and bond stress-slip relation proposed by Mobasher [15]*

This constitutive law for bond stress-slip behavior results in the bond stress and yarn force distributions shown in Figure 9. The different stages are discussed hereafter.

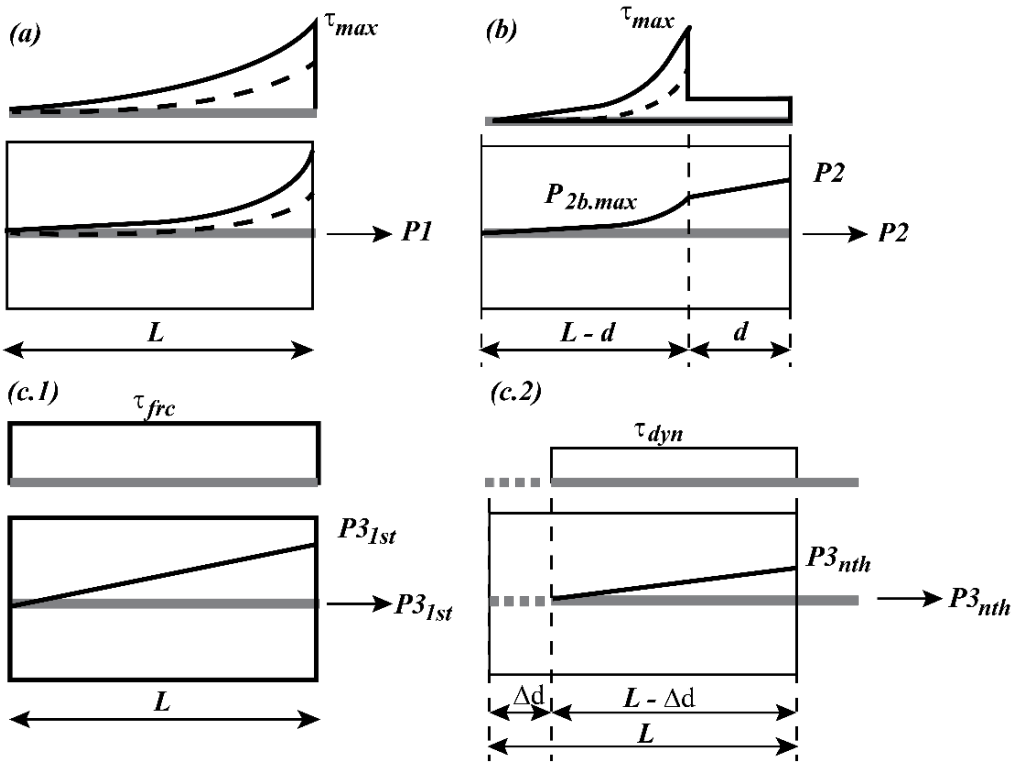

Figure 9 *Bond stress and force distribution for a) elastic stage b) non-linear stage with partial debonding, and c) rigid body motion [15]*

a. 1st regime – elastic stage

This first slip regime $s_1(P_1)$, as described by Eqs. (3.1) to (3.3), is characterized by a linear yarn pull-out behavior resulting from the linearly increasing bond stress (i.e. constant bond stiffness κ) up to the yarn force $P_{1b,max}$:

$$s_1 = \frac{P_{1b,max} Q}{\beta \sinh(\beta L_b)} [\cosh(\beta L_b) - 1] \tag{3.1}$$

$$P_{1b,max} = \frac{\tau_{max} \psi}{\beta} \tanh(\beta L_b) \tag{3.2}$$

with $\tau_{max} = \kappa s_1$ (3.3)

and where

$$\beta = \sqrt{\psi \kappa Q} \tag{3.4}$$

$$Q = \frac{1}{\eta E A_f} + \frac{1}{E A_m} \text{ with } \eta < 1 \tag{3.5}$$

ψ is the outer perimeter of the yarn while Q is a stiffness ratio coefficient of mortar and textile. If the material properties (provided by the manufacturer, e.g. see Table 1) for the fibers are used in reverse computing, the normal force stiffness of the yarn EA_f has to be reduced by the bond efficiency coefficient η. It considers that not all filaments in the yarn are activated, due to the lack of bonding for all filaments (that is, the mortar is not penetrating to the innermost core of the yarn and the yarn is not totally saturated by resin, also see Figure 2). This reduction of axial stiffness is often referred to as sleeve effect. Furthermore, this efficiency coefficient also considers the initial curvature in the yarns (from execution tolerances and weaving), leading to a reduced axial stiffness.

Thus, the reduction coefficient η represents the stiffness efficiency of the bonded yarn, considering different kind of deficiencies, in comparison to the uniaxial tensile behavior of the yarn alone. In other words, the efficiency coefficient is given by

$$\eta = \frac{\sigma_{f,u}}{f_{t,u}} = \frac{A_{eff}}{A_{tot}} \tag{3.6}$$

where A_{eff} is the area of the embedded yarn effectively activated for yarn stiffness. It is not applicable to the free length of the yarn (if any free length is available in the experimental test setup) or another (higher) value for η needs to be considered on that free length.

In the calibration of values for the bond model parameters from experimental results of pull-out tests, which provide the global force-slip behavior for a given bond length L_b, the unknown parameters are:

- κ – elastic bond stiffness
- τ_{max} – maximum bond stress in first bond regime
- η – efficiency coefficient

Eqs. (3.1) to (3.3) allow to determine two unknown parameter values and thus, one of the three unknowns must be selected or a third equation must be identified, respectively. Input for parameter value calibration is obtained by (visually) choosing the values of $P_{1b,max}$ and s_1 from the experimental pull-out response. Dividing Eq. (3.2) by Eq. (3.1) results in Eq. (3.7) which is solved for β to calculate the value of κ from Eq. (3.4), assuming a given value for η in Eq. (3.5).

$$s_1 = \frac{P_{1b,max} Q}{\beta \sinh(\beta L_b)} [\cosh(\beta L_b) - 1] \tag{3.7}$$

Note that the efficiency coefficient of carbon yarns is approximately η = 0.20 but can vary considerably, depending on the shape of the yarn [3], also see Table 2 for other materials. The elastic bond stiffness κ being identified, the maximum elastic bond stress τ_{max} can then be found from Eq. (3.3) with the chosen slip s_1. The limit of this first bond regime is attained when the maximum bond stress τ_{max} is reached at the loaded end which is equivalent to attaining $P_{1b,max}$. Due to the hyperbolic force distribution – resulting from the linear bond stress-slip constitutive law – the available bonded length L_b is completely activated, anyway, see Figure 9 (a) and Eq. (3.2).

b. 2nd regime – non-linear stage

This bond regime is characterized by an increasing “debonded” length d penetrating from the loaded end into the available anchorage length L_b, see Figure 9 (b). However, the yarn is not completely debonded on this length d but it still contributes to the anchorage strength by a frictional bond stress τ_{frc}. The maximum pull-out strength $P_{2,max}$ is determined by superposition of the contributions of the elastically bonded zone with length $L_b - d$, resulting in a force $P_{2b,max}$, and of the debonded zone with a linear force increase P_d, resulting from the constant bond stress τ_{frc}:

$$P_{2,max} = P_{2b,max} + P_d \tag{3.8}$$

where

$$P_{2b,max} = \frac{\tau_{max} \psi}{\beta} \tanh\big(\beta(L_b - d)\big) \text{ and} \tag{3.9}$$

$$P_d = \tau_{frc}\, \psi d \tag{3.10}$$

The slip s_2 at the loaded end of the yarn at attaining pull-out strength $P_{2,max}$ is given by

$$s_2 = \frac{P_{2b,max} Q [\cosh(\beta(L_b - d)) - 1]}{\beta \sinh\big(\beta(L_b - d)\big)} + \frac{1}{2} Qd\big(P_{2,max} + P_{2b,max}\big) \tag{3.11}$$

The values of $P_{2,max}$ and the associated slip s_2 in this second regime are again determined from the experimental pull-out response. In solving Eqs. (3.8) to (3.10), the unknowns are:

- τ_{frc} – frictional bond stress
- d – debonded length

and thus, there are enough equations to determine the unknown parameter values. The frictional bond stress τ_{frc} can be calculated from

$$\tau_{frc} = \frac{P_{2,max} - P_{2b,max}}{\psi d} \tag{3.12}$$

The maximum anchorage strength $P_{2,max}$ is attained for values of $d < L_b$. When d attains the available anchorage length L_b, corresponding to the state shown in Figure 9 (c.1), the yarn force is already in the post-peak domain. The associated slip limit s_2, see Figure 8, can also be determined from Eq. (3.11). The analytical determination of the debonded length d is further discussed in 3.2.4.

c. 3rd regime – rigid body motion

This behavioral stage is of little practical importance as the yarn force is already far in the post-peak unloading branch. In this stage, the yarn is being pulled-out from the mortar matrix, see Figure 9 (c.2), thereby reducing the available bond length. Only the dynamic bond stress τ_{dyn}, assumed lower than the frictional bond stress τ_{frc}, see Figure 8, provides a still available pull-out strength. The force in the yarn can be calculated from

$$P_{3,nth} = \tau_{dyn}\psi(L_b - \Delta d) \tag{3.13}$$

where Δd is the pulled-out length at the unloaded end. The associated slip s_3 follows from

$$s_3 = Q\left[\tau_{dyn}\,\psi\left(L_b\Delta d - \frac{{L_b}^2}{2} - \frac{\Delta d^2}{2}\right) + P_{3,nth}(L_b - \Delta d)\right] \tag{3.14}$$

Note that this slip results from the applied force only. To calculate the total slip of the yarn, the slip s_2 at attaining pull-out strength $P_{2,max}$ and the value of Δd have to be added to s_3:

$$s_{tot} = s_2 + s_3 + \Delta d \text{ for } s > s_2 \tag{3.15}$$

3.2.2 Bond behavior of multiple yarns – Maeder's dimensioning model

Based on data from literature and own experimental results, Maeder [18] developed a proposal for a dimensioning model for the anchorage capacity of textiles bonded to mortar, based on Mobasher's bond model for a single yarn, targeting the influence of textile width and the number of textile layers. Tolerances in test specimens (free textile length) in combination with the chosen test setup (push-pull double lap) did unfortunately not allow to evaluate the impact of the number of textile layers. Due to these tolerances, one of the multiple layers could already be pulled-out while the further layers are not or not fully activated yet.

Maeder limited his own experimental investigations to textiles made of carbon fibers. For other textile materials and also multiple textile layers, data from the literature is used. It is shown that the dimensioning model exposed hereafter can also be applied to these cases.

3.2.3 Experimental study

Maeder [18] conducted an experimental campaign in which 24 specimens of constant bond length but with four different carbon fiber textile widths combined with one to three grid layers were tested in a push-pull double lap test setup, measuring the applied force, overall displacements and local yarn slips. To measure local yarn slips, Digital Image Correlation (DIC) was used.

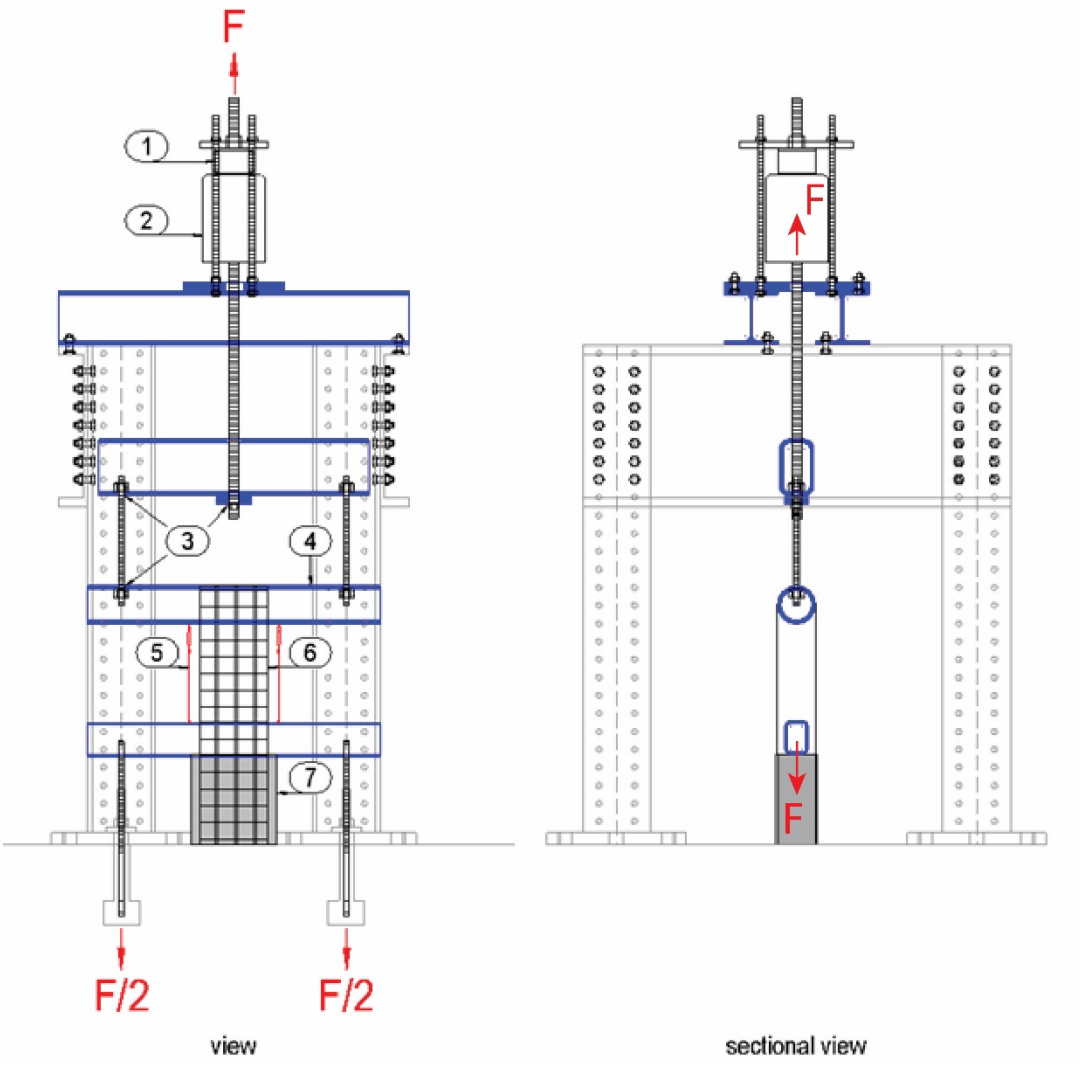

Figure 10 *Test rig for push-pull double lap tests [18]*

The test specimens were produced by attaching the textile grids on the surface of the concrete elements using layers of 5-10 mm of sprayed mortar. After curing, the specimens were tested in a push-pull double lap test setup (Figure 10).

The failure observed in the first tests was a tensile failure of the grid, implying that the bond length was so long that the tensile capacity of the grid could be completely anchored and thus, the bond length was too long for testing bond behavior. Therefore, it was successively reduced until slip failure was attained.

The three-layer specimens showed a substrate failure thus no behavioral analysis could be later performed for grid bond, either. In the end, pull-out failure could be reached for eleven of the initial 24 specimens.

The pull-out responses [18] are illustrated hereafter in global force-displacement and average force-strain per yarn diagrams for specimens with bond widths of 30 cm (Figure 11), 60 cm (Figure 12) and 90 cm (Figure 13), all with a bond length of 7.5 cm.

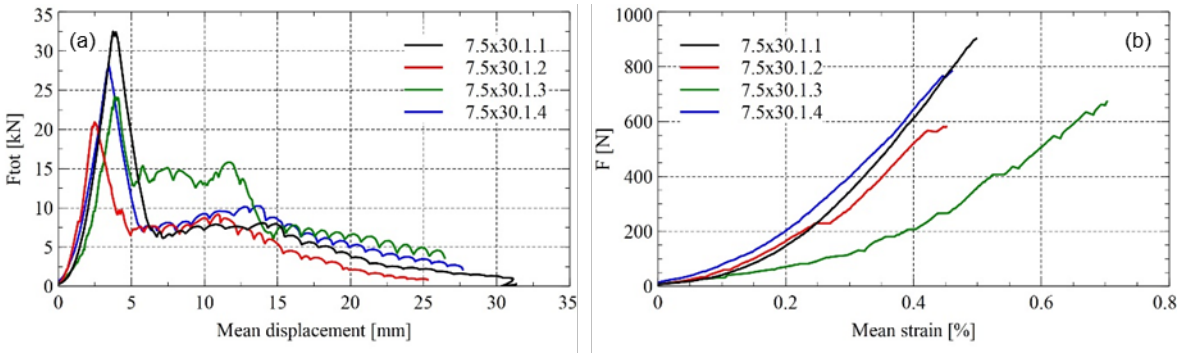

Figure 11 *Experimental results for bond length L_b = 7.5 cm and bond width B = 30 cm – (a) total force to mean displacement, and (b) average force per yarn to average strain*

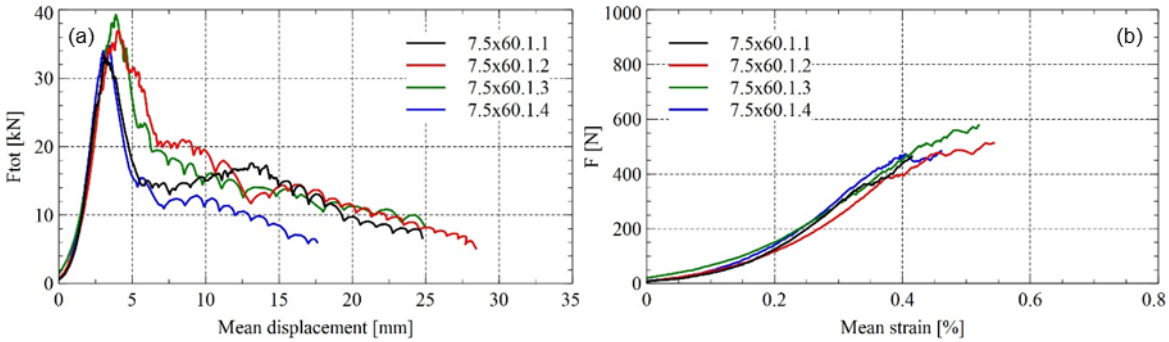

Figure 12 *Experimental results for bond length L_b = 7.5 cm and bond width B = 60 cm – (a) total force to mean displacement, and (b) average force per yarn to average strain*

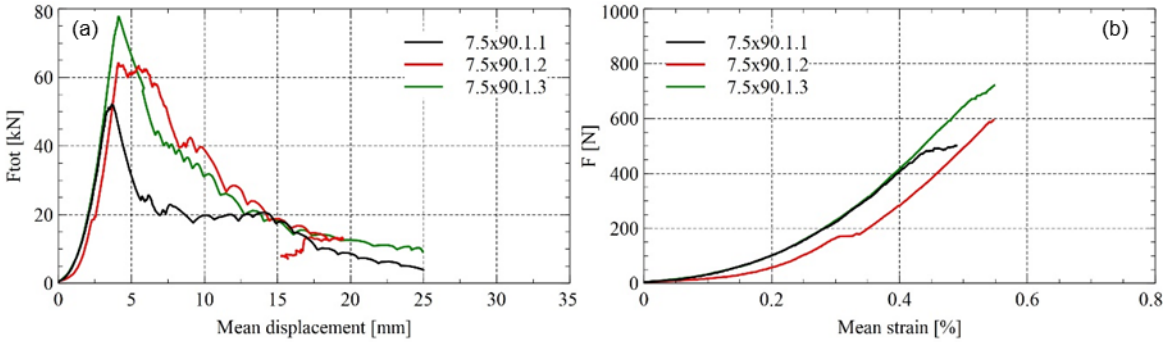

Figure 13 *Experimental results for bond length L_b = 7.5 cm and bond width B = 90 cm – (a) total force to mean displacement, and (b) average force per yarn to average strain*

3.2.4 Model parameter value calibration

Using the experimental forces and displacements, measured material properties as well as local yarn slips determined by DIC, values for the parameters of Mobasher's model (e.g. κ, η, and d) could be calibrated, further allowing to compute analytical bond stress-slip constitutive laws as a function of the textile width (Figure 14). The calibration approach consists of 12 steps and is based on the model parameters shwon in Table 3. It is principally applicable for any textile material type.

Table 3 *Summary of model parameters*

Input values	Calibrated parameters	Dependent parameters
ψ	η	Q
s_1	κ	β
s_2	d	τ_{max}
P_1		τ_{frc}
P_2		

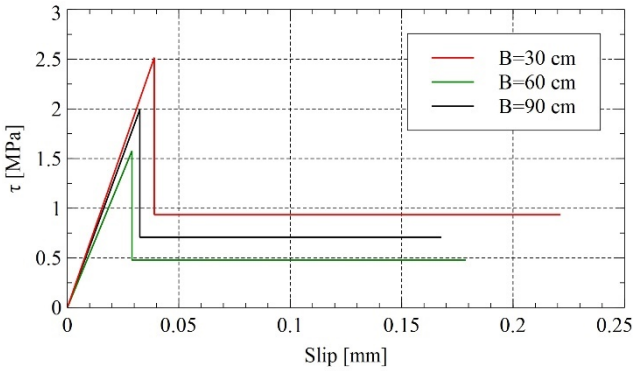

Figure 14 *Calibrated average bond stress-slip relationships for bond widths of 30 cm, 60 cm, and 90 cm, respectively (valid for S&P carbon textile [18])*

1. Identify material properties (Table 4 for S&P carbon textiles)
2. (Visually) determine slips s_1 and s_2 and associated forces $P_{1b,max}$ and $P_{2,max}$ from the experimental response
3. Calculate $P_{1b,max}/s_1$ from experimental values
4. Set starting value of η (e.g. η = 0.20-0.25, Table 2) and calculate Q from Eq. (3.5)
5. Define κ in Eq. (3.7) such that the calculated ratio $P_{1b,max}/s_1$ from step 3) is attained
6. Calculate β from Eq. (3.4)
7. Calculate τ_{max} from Eq. (3.3)
8. Define $d < L_b$ in Eq. (3.11) such that s_2 is equal to the measured slip at maximum force
9. Calculate τ_{frc} from Eq. (3.12)
10. If $d > L_b$, redefine η in 4) and go through further steps again
11. Check if chosen η and d are correct by deriving Eq. (3.8) for d

$$P_{2,max}(d)' = 0 = -\tau_{max}\psi sech^2\big(\beta(d - L_b)\big) + \psi\tau_{frc} \tag{3.16}$$

Then, calculate $P_{2,max}$ from Eq. (3.8). The difference between calculated force and that from step 2) must be zero.

12. If $\Delta P_{2,max} = 0$, then values for η, κ and d are correct and all parameters are defined. If not, restart at step 4)

Table 4 *Material properties*

Parameter	Symbol	Value	Unit
Yarn cross-section	$A_{f,i}$	1.79	mm²
Yarn elastic modulus	E_f	240	GPa
Yarn circumference	ψ	9.33	mm
Mortar cross-section	A_m	425	mm²
Mortar elastic modulus	E_m	26	GPa
Bond length	L_b	75	mm

3.2.5 Influence of bond width

The main objective of Maeder's work was to investigate the impact of bond width on the anchorage capacity or pull-out strength as a function of bond width, respectively. A further objective was to evaluate the impact of the number of textile layers on bond capacity but, as exposed above, this could not be evaluated in more detail. The pull-out strength also depends on the force distribution across the grid. If the yarn force at the edges is higher than in the middle of the grid, for example, the assumption of a constant grid stress distribution $\sigma_{f,m}$ can be misleading in determining the bond capacity, Figure 15.

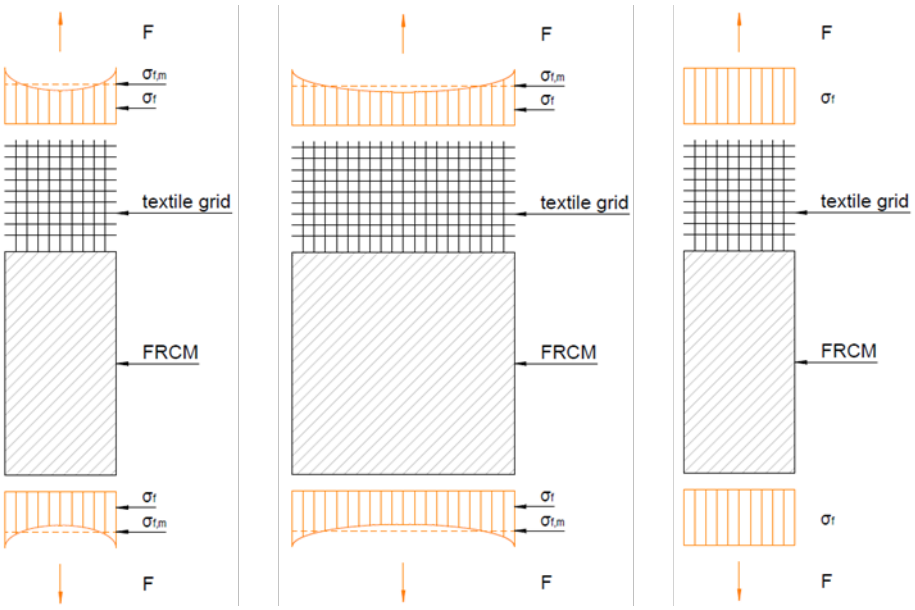

Figure 15 *Stress distribution of a narrow grid, a large grid and constant stress distribution [18]*

For three test specimens, digital image correlation (DIC) was used to determine individual yarn forces (by using individual experimental strains and the elastic modulus) as well as anchorage slips.

These results show that the force per yarn is quite randomly distributed across the width, Figure 16. This may also be due to tolerances in the test set-up: if the steel profile for load introduction is not perfectly perpendicular to the grid, not all yarns are activated at the same time. It is also possible that not all yarns have the same initial length l_0 due to test specimen fabrication tolerances.

All this results in a non-uniform yarn force distribution. In contrary to the randomly distributed yarn forces, the local bond behavior of a single yarn depends on the local mortar properties and is therefore independent of the bond width.

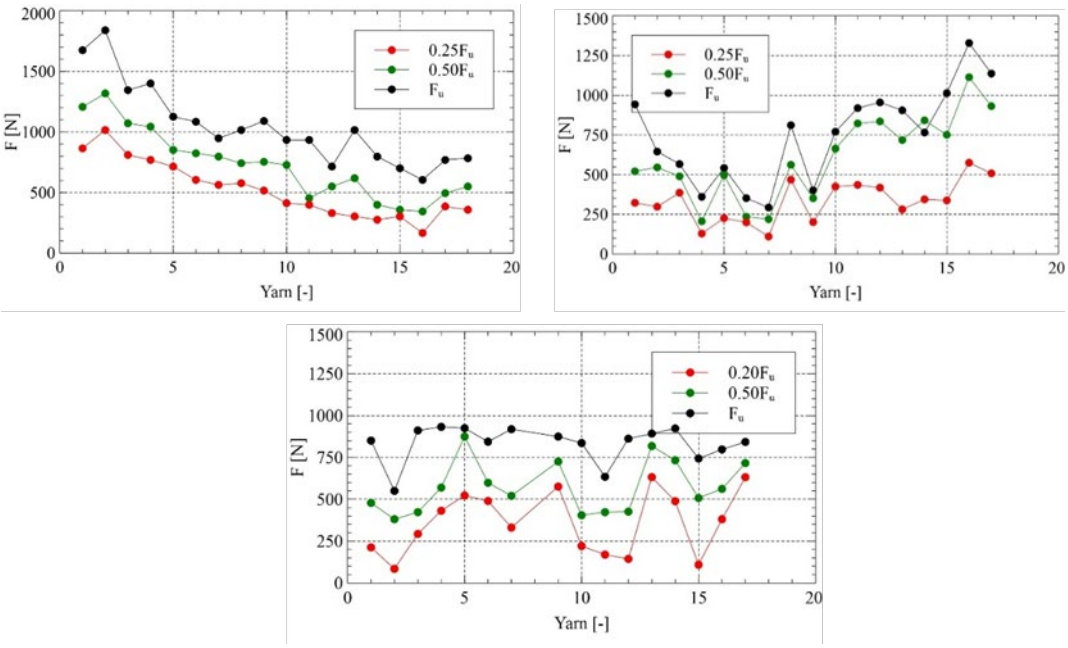

Figure 16 *Force distribution of three specimens at different load levels [18]*

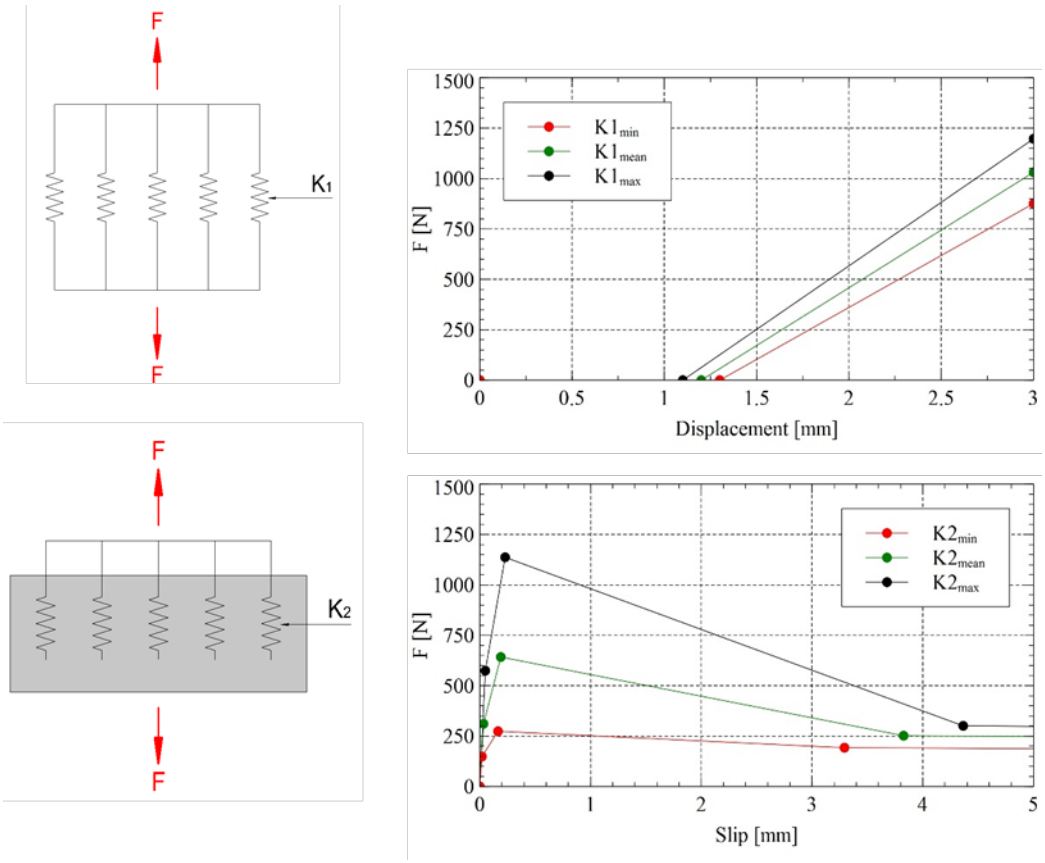

Figure 17 *Spring models [18]*

The influence of the textile width on pull-out strength of grids was therefore investigated analytically with the help of two spring models (Figure 17).

These spring models represent the impact of the free textile length (spring stiffness K_1) as well as the influence of the bonded length (spring stiffness K_2), resulting from the calibrated bond stress-slip relationships, on the global force-displacement behavior. Both springs consider a possible variation of the associated properties by using average and extreme 5th and 95th percentile values.

The spring stiffness K_1, describing the yarn behavior, can be calculated from Eq. (3.17):

$$K_1 = \frac{\omega_{el} E_f A_{f,i}}{l_0} \tag{3.17}$$

where ω_{el} is a global stiffness efficiency coefficient and l_0 is the free length of the textile. Furthermore, length tolerances of the yarns are considered by a varying initial displacement needed to activate the yarn stiffness (Figure 17) which is later transferred to the anchorage zone as an initial slip.

The spring model K_2, describing the bond behavior of a single yarn without initial slip, can be derived from Figure 18, considering the possible variations of the implied parameters (Table 5) and using the expressions exposed in 3.2.1. The descending post-peak branch was introduced to integrate the rigid body motion (Figure 17). The associated dynamic bond strength τ_{dyn} was estimated from the global force-displacement curves.

Table 5 *Values considered in determining spring stiffness K_2*

	η [-]	κ [N/mm³]	d [mm]	τ_{max} [MPa]	τ_{frc} [MPa]	τ_{dyn} [MPa]	s_1 [mm]	s_2 [mm]	β [1/mm]	Q [10^{-6}/N]
5%	0.17	44	52	1.20	0.28	0.28	0.020	0.165	0.076	13.8
50%	0.34	61	56	2.09	0.74	0.34	0.034	0.190	0.063	6.93
95%	0.51	80	60	3.64	1.30	0.41	0.050	0.229	0.059	4.65

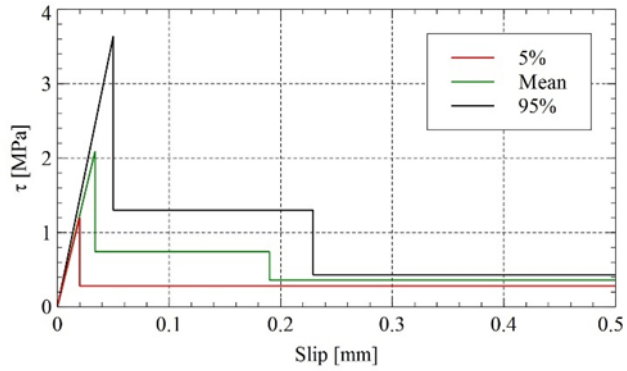

Figure 18 *Bond stress-slip relations (valid for S&P carbon textile [18])*

As the values for determining K_2 are derived from experimental responses (DIC), they are already influenced by the variable stiffness of the yarns (K_1). This is why K_2 is a spring connected in parallel series considering the force variation of the yarns but the bond of one yarn anchorage. The stiffness of the yarn has no impact on the local bond behavior and thus, the values of K_2 can be randomly distributed and connected with the variable initial displacements of the spring K_1 representing the free length of the textile grid.

It is chosen to combine $K_{2,min}$ with the maximum initial displacement of K_1 as an initial slip, and $K_{2,max}$ with the minimum initial displacement, in order to consider extremes and to simplify further calculations. The ultimately resulting spring model for one yarn anchorage is depicted in Figure 19.

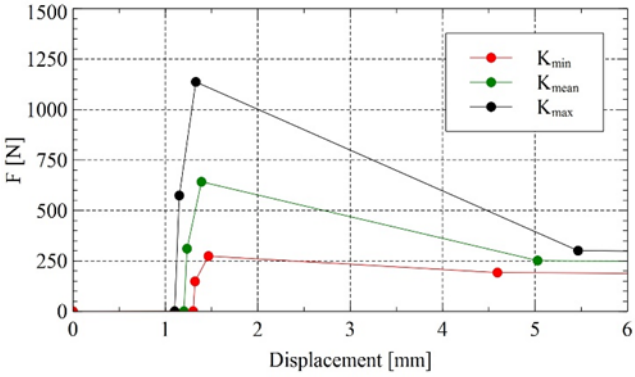

Figure 19 *Spring model for one yarn anchorage [18]*

To determine the influence of bond width on the pull-out strength, multiple yarns have to be randomly described with bond stress-slip relationships as in Figure 19. All these anchorage springs have to be connected in parallel to obtain an equivalent anchorage stiffness of a grid with a given width:

$$K_{grid} = \sum_{i}^{n} K_i \tag{3.18}$$

The stiffness K_{grid} is calculated for 18, 36, 54, 72 and 90 yarns in parallel, representing bond widths of 30 cm, 60 cm, 90 cm, 120 cm and 150 cm, respectively (for a grid with yarn spacing as applied in the tests). The force-slip curve for the anchorage of these grids is determined, followed by adding the elastic deformation of the yarns as a function of K_1, to obtain global force-displacement curves. As shown in [18], this approach can reproduce quite accurately experimental responses of applied force and average displacement.

Such calculations of K_{grid} and of global force-displacement curves are repeated 20 times in which randomly selected distributions of anchorage and free length stiffnesses are combined. This procedure allows obtaining global “virtual” test results based on the bond stress-slip relationships that were calibrated from local slip measurements.

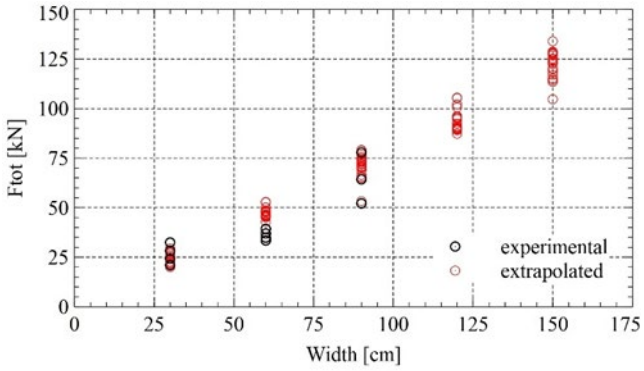

Figure 20 *Total force of extrapolated and experimental results as a function of bond width [18]*

Figure 20 shows these "virtual" and experimental results in terms of maximum force against bond width, confirming a good agreement between the applied approach and experimental observations.

By dividing the total maximum force by the associated total cross-section of the textile, an average effective textile stress as a function of bond width is obtained, see Figure 21. It can be seen that, on average, there is hardly any bond width effect even if the yarn force distribution is not constant across the grid width. Note that average textile stresses are approx. 800 MPa, reasonably confirming the recommended value of η = 0.20 for carbon textiles (Table 2).

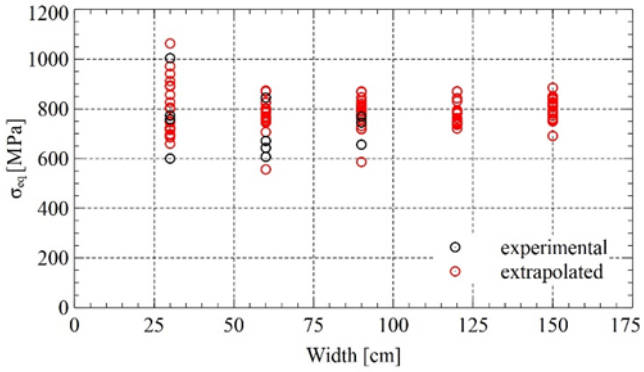

Figure 21 *Equivalent yarn stress of experimental and extrapolated results [18]*

Still, it can be observed that the obtained yarn forces vary more for narrow grids than for larger grids. This is related to the number of yarns and the random attribution of spring properties. For a smaller number of yarns, it is more probable that a majority of yarns are either described with K_{min}, K_{mean} or K_{max} than for a larger number of yarns (stochastic behavior, multiplication rule).

If characteristic values (5th percentile) textile stresses would be considered, a certain effect of bond width on average textile stress could be noted for small grid widths. However, as textile widths below 50 cm are of little practical importance for strengthened deck slabs, the effect of bond width on transverse textile stress distribution can be neglected for further investigations.

3.2.6 Dimensioning model

The pull-out strength of a single yarn can be computed from superposing Eqs. (3.9) and (3.10). The resulting Eq. (3.19) can also be applied to calculate the pull-out strength of a textile grid as the bond width approximately has a linear influence, that is, for practically relevant textile widths (Figure 21):

$$P_{2,max} = \frac{\tau_{max}\psi}{\beta}\tanh\big(\beta(L_b - d)\big) + \tau_{frc}\psi d \tag{3.19}$$

with β from Eq. (3.4). According to Maeder [18], the bond stress levels can be defined as

$$\bar{\tau}_{max} = C_1 f_{ctm} \tag{3.20}$$

$$\bar{\tau}_{frc} = C_2 f_{ctm} \tag{3.21}$$

Thus, in analogy to steel reinforcing bars, Maeder proposes to refer to the average tensile strength of the mortar matrix, which masters the bond strength of such rather smooth yarns and is defined as a function of the compressive strength:

$$f_{ctm} = 0.3 f_{ck}^{2/3} = 0.3(f_{cm} - 8)^{2/3} \tag{3.22}$$

Maeder further proposes that the slope κ of the bond stress-slip constitutive law should be related to the mortar's elastic modulus, assuming that, in the elastic stage, the yarn is perfectly bonded to the mortar. Due to the yarn's high axial stiffness, associated slips are primarily a consequence of the shear deformations in the surrounding mortar which, in turn, can be directly related to its elastic modulus. Therefore, κ can be described as

$$\bar{\kappa} = C_3 f_{cm}^{1/3} \tag{3.23}$$

The length *d*, with a reduced but constant bond stress τ_{frc}, depends on the anchorage length and has to be limited for longer anchorage lengths, as a function of stiffness parameter β [18], thereby limiting the maximum anchorage capacity. This length *d* is given by

$$d = 0.75 L_b \leq \frac{40\ mm}{1 - 6.9\beta} \tag{3.24}$$

The efficiency coefficient η – to be considered in the determination of the stiffness ratio $Q = \big(\eta E A_f\big)^{-1} + (E A_m)^{-1}$, Eq. (3.5) – is assumed as a function of the textile fiber material (Table 2):

- Carbon $\eta = 0.20$
- AR-Glass $\eta = 0.25$
- Basalt $\eta = 0.25$

The average pull-out strength of a grid then becomes

$$F_{Rm} = n\left[\psi 0.3 f_{ck}^{2/3}\left(\frac{C_1}{\beta}\tanh\big(\beta(L_b - d)\big) + C_2 d\right)\right] \tag{3.25}$$

where $n = b/e_f$ is the number of yarns for a given textile width *b* with yarn spacing e_f, as well as $\beta = \sqrt{\psi\kappa Q}$ from Eq. (3.4) with yarn bond perimeter ψ and *Q* from Eq. (3.5).

Table 6 shows the proposed values for parameters C_1 to C_3 at different analysis levels [18].

Table 6 *Coefficient values in Maeder's model [18] for different structural analysis levels*

Average	Characteristic	Design
$C_1 = {}^2/_3$	$C_1 = {}^1/_2$	$C_1 = {}^1/_2$
$C_2 = {}^1/_4$	$C_2 = {}^1/_6$	$C_2 = {}^1/_6$
$C_3 = 16.9$	$C_3 = 11.1$	$C_3 = 10.5$
$\gamma_M = 1.0$	$\gamma_M = 1.0$	$\gamma_M = 1.5$

Maeder [18] also compared results from his analytical proposal to some 130 experimental results from other literature studies, with different fiber materials (carbon, PBO, glass, basalt) and variable number of textile layers (1-3 layers). With the proposed values, exact agreement of theoretical and experimental values is found on average, with a coefficient of variation of 22% that can be considered satisfactory, recalling the dependency of many parameters on the mortar tensile strength.

3.3 Mechanical anchorage

In general, textile anchorage by bond only is preferred in strengthening projects, for economic and execution time reasons. Yet, in particular situations, mechanical anchorage may be applied to improve the efficiency of the textile reinforcement anchorage.

There are multiple mechanical anchorage systems commercially available that can be used for fixing the strengthening textile to the element to be strengthened. These anchorage devices are made of steel pieces, around which the textile meshes are wrapped, and which are fixed with steel anchor bolts in the concrete support. One example is the system commercialized by S&P (Figure 22).

These anchorage rails have rounded edges to reduce transverse pressure on the fragile fiber grids, being very sensible to this kind of loading. The capacity of such mechanical anchorage systems is, in general, a multiple of the anchorage by bond, and allows the full exploitation of the textile capacity if the support is sufficiently strong to provide the necessary anchor bolt capacity.

Figure 22 *S&P mechanical anchorage system [19]*

3.4 Interface between TRC and concrete support

The behavior of the interface between textile reinforced concrete and a concrete support mainly depends on the treatment of the surface before application of TRC.

Before applying a first layer of mortar, the concrete support must be roughened, preferably by hydro-demolition (possibly by abrasive devices). After this treatment and cleaning of the surface, the water content of the support surface needs to be increased such that the water in the mortar mix is not absorbed by capillary suction of the support, resulting in insufficient hydration and reduced mechanical properties of the mortar. If this preparation is done correctly, no failure at the interface between mortar and concrete should occur, which is confirmed by the absence of this potential failure type in the studied data.

4 Database evaluation for suitability of analytical dimensioning approaches

4.1 Database

This research project started with a data gathering campaign from the literature [3], [5], [6], [20]-[33], assembled in a database which has more than 150 entries from which about 50 refer to unstrengthened reference specimens. In most of the test series, the tested specimens were reinforced concrete beams while one-way slab elements were less often used. In somewhat more than ten cases, U-wrap strengthening on beam elements was applied on the full length of the element. These test results were discarded since this evaluation investigates flexural strengthening of slab elements.

For each entry, the database contains 58 different parameters like span, cross-sectional geometry, material properties and experimental results. In some cases, parameters like Young's modulus of the steel reinforcement or the mortar tensile strength were not given in the reference. In such cases,tThese were determined by computing (e.g. tensile strength as a function of compressive strength, Eq. (2.1)) or by assuming them based on the other given properties. Table 7 presents the database entries per textile material and reported failure types.

Table 7 *Types of failure per material*

Material	Carbon	PBO	Basalt	Glass	Total
Number of tests	33	45	14	8	100
Delamination	12	28	1	2	43
Slippage	15	15	11	2	43
Fiber rupture	6	-	2	4	12
Concrete crushing	-	2	-	-	2

4.2 Empirical evaluation

A first evaluation looks at the flexural capacity increase of a test specimen thanks to TRC, regardless of textile material or failure type. Figure 23 shows that, on average, each applied textile layer increases the flexural capacity at Ultimate Limit State (ULS) by 20-25%, for configurations with up to four layers of textile. For more than four layers, the effectiveness of the textile reinforcement seems to be affected, yet only few database entries had five textile layers or more.

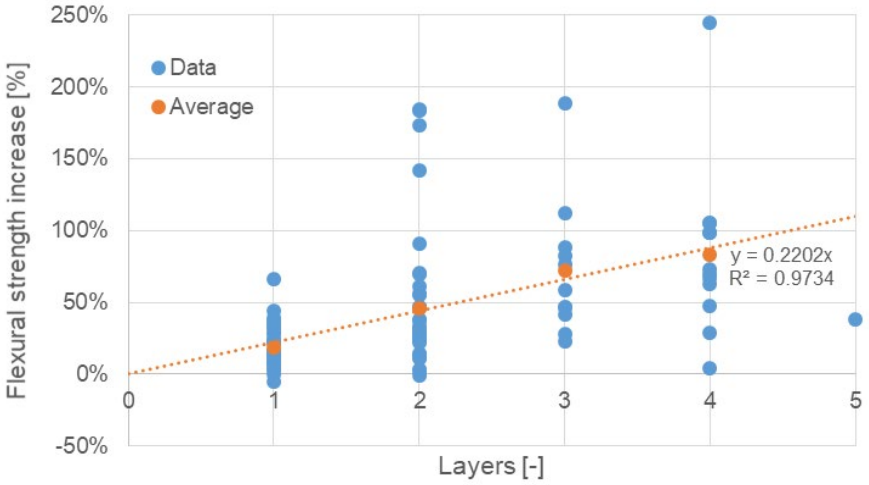

Figure 23 *Empirical flexural capacity increase at ULS from database entries*

Further looking at the failure type as a function of the number of textile layers, it turns out that delamination occurs more often in multiple layer configurations while slippage or anchorage failure, respectively, is specific to configurations with one or two textile layers.

4.3 Suitability evaluation of structural analysis approaches

Various analytical approaches were evaluated for suitability, using the given input parameters and comparing their output results to the experimental failure loads.

4.3.1 Rigid bond approach

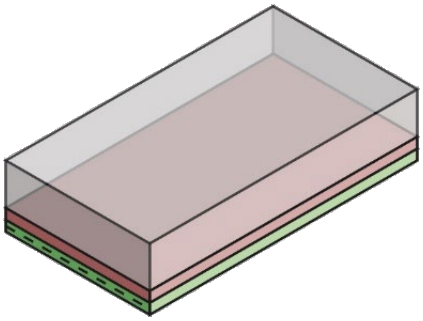

This approach considers the assumptions of classic reinforced concrete theory assumptions, that is, plain sections remain plane, concrete tensile strength is neglected, reinforcement elements (steel bars and textile) bear axial forces only, and bond between reinforcement and concrete or mortar is considered rigid, respectively.

Sectional forces at Ultimate Limit State (ULS) are determined from equilibrium and strain compatibility conditions between concrete in compression and steel and textile reinforcement in tension, further considering a maximum ultimate strain for the concrete in compression of 3‰ and using a simplified stress block for determining concrete stress [34]. Stresses in the reinforcements are determined from associated constitutive laws (Figure 3). The behavior of the steel reinforcement is considered linear-elastic, perfectly plastic; hence, hardening is neglected due to the considerable axial stiffness reduction after yielding in comparison to that of the textile remaining elastic.

The position of the neutral axis is determined using a solver to satisfy normal forces equilibrium (Figure 24). The theoretical flexural capacity can then be determined from the internal forces and their position in the cross-section and is compared to the experimental capacity at failure.

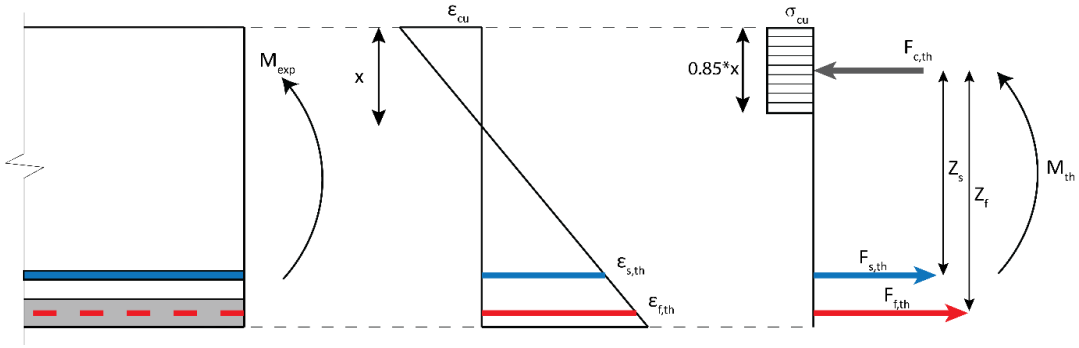

Figure 24 *Rigid bond approach*

In a first step, the strengthening textiles are considered as a perfectly bonded linear elastic reinforcement, that is, neglecting the yarn efficiency (Table 2). The comparison between the experimental and theoretical bending moments M_{exp} and M_{theo}, respectively, shows that the experimental capacity of the strengthened elements is largely overestimated (Figure 25). It is found that in 80% of the cases, the experimental capacity is overestimated by 18% on average, with a coefficient of variation (COV) of 30% (Table 8) for normal distribution. Thus, disregarding the efficiency coefficient η leads to overestimating the real capacity and unsafe results.

Therefore, the approach is refined in a second step by considering efficiency coefficients (Table 2) in computing the flexural capacity by reducing the axial stiffness of the textile with η. This refinement results in a clear underestimation of the true capacity by 20% on average and a somewhat reduced COV of 26% (Table 8). Yet, only 25% of the theoretical results overestimate the real capacity.

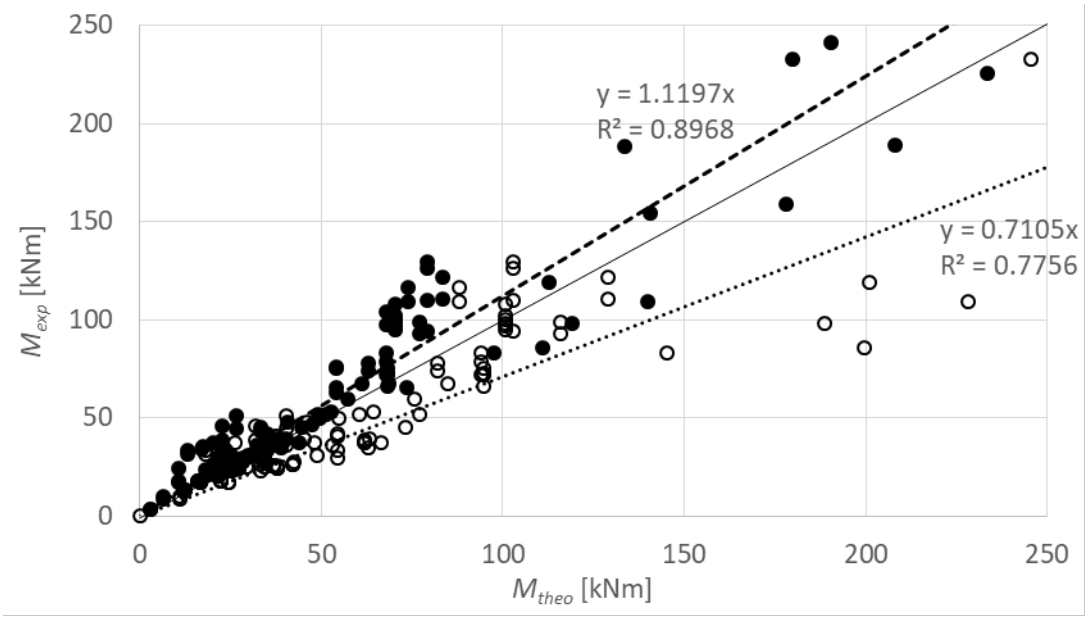

Figure 25 *Comparison of experimental and theoretical results for rigid bond approach, with (data points with ●) and without (data points with ○) consideration of* η

Table 8 *Statistics of rigid bond approach*

	M_{exp} / M_{theo} (η = 1)	M_{exp} / M_{theo} (η = 0.20..0.25)
AVG	0.85	1.20
COV (ND)	30%	26%

However, since the majority of the tested specimens did not fail by rupture of the fibers, the theoretical strain cannot be compared to the ultimate strain of the fibers to determine real efficiency coefficients, as the reference strain for other failure types (i.e. delamination, slippage) is a priori unknown. As this approach provides results with relatively high safety margins and still considerable COV, rigid bond between textile and mortar proved to be an unreliable assumption, rendering the strain compatibility condition impractical.

4.3.2 Unbonded end-anchored textile reinforcement

Opposed to the main assumption of the previous approach, no bond between textile and mortar, at ULS, is considered here over a certain length L_{ef} of the strengthened specimen but the textile is presumed to be anchored at both ends, in the remaining length of the strengthening layer.

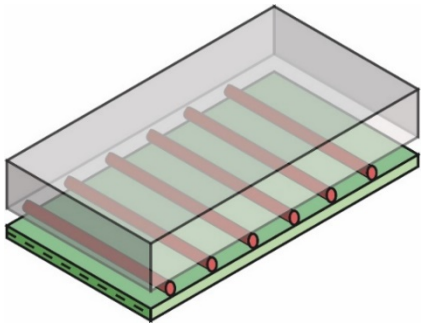

Assuming a rigid body failure mechanism (Figure 26), the strain in the textile can be computed from the experimental deflection δ_u attained at maximum experimental bending moment. Using this ultimate deflection, a rigid body rotation is computed which is translated into a total elongation of the linear-elastic textile.

To determine the effective textile strain, this total elongation is divided by an effective length L_{ef} on which this total elongation occurs. The appropriate effective length is yet to be determined. The first choice was the length where the concrete element is cracked, thus assuming that the textile is anchored in the uncracked part of the strengthening layer.

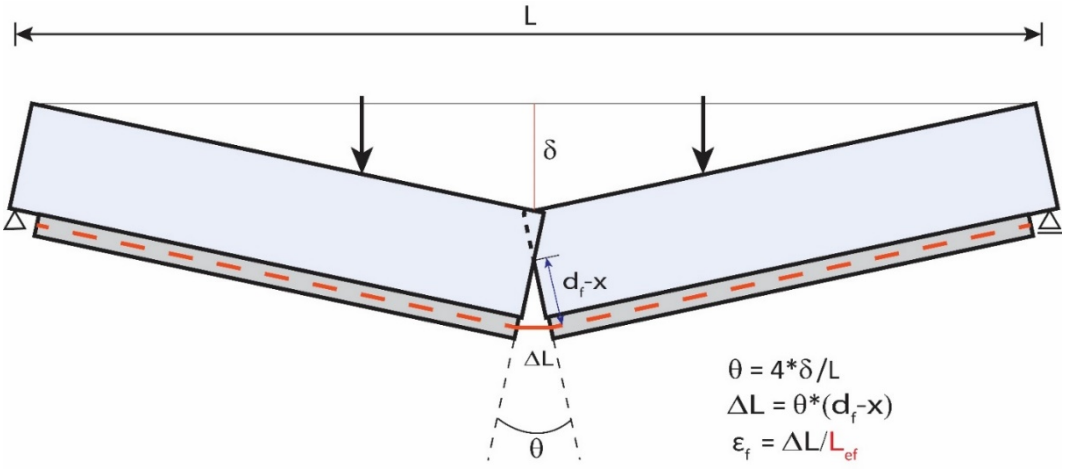

Figure 26 *Mechanics of unbonded end-anchored approach*

4.3.3 Anchorage length for strengthening textile

The available textile anchorage length, also at ultimate limit state, in slabs with flexural strengthening made of TRC depends mainly on the position of the cracking moment. This length is computed as the distance between the end of the TRC strengthening layer and the first crack (Figure 27).

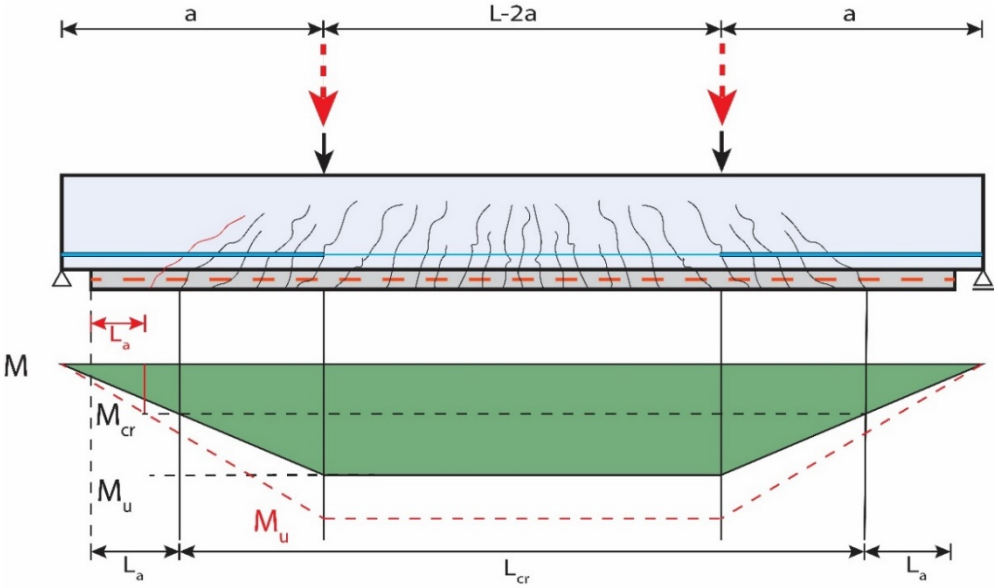

Figure 27 *Influence of the M_u on the anchorage length L_a*

In the evaluation of experimental results on test specimens subjected to 4-point bending, the position of the first crack at failure of the specimen depends on two parameters: the maximum bending moment M_u which, in turn, depends on the ultimate test load and the distance a between support and load application, as well as the mortar tensile strength which is used to compute the cracking moment M_{cr}. The theoretically uncracked length, available for textile anchorage, can be computed as

$$L_a = \frac{M_{cr}}{M_u} a' \tag{4.1}$$

where *a'* is determined by subtracting the unstrengthened length near the support from the shear span *a*. In evaluating the compiled database, it could be observed that the M_{cr}/M_u ratio can vary considerably due to different mortar characteristics and test setups (that is, shear span *a*).

4.3.4 Cracked length

To compute the theoretically cracked length, it is necessary to know the cracking moment of the strengthened (composite) section and to find its position in the moment diagram (Figure 28). The cracking moment is computed using the tensile strength of the mortar and further considering the influence of the textile and steel reinforcement.

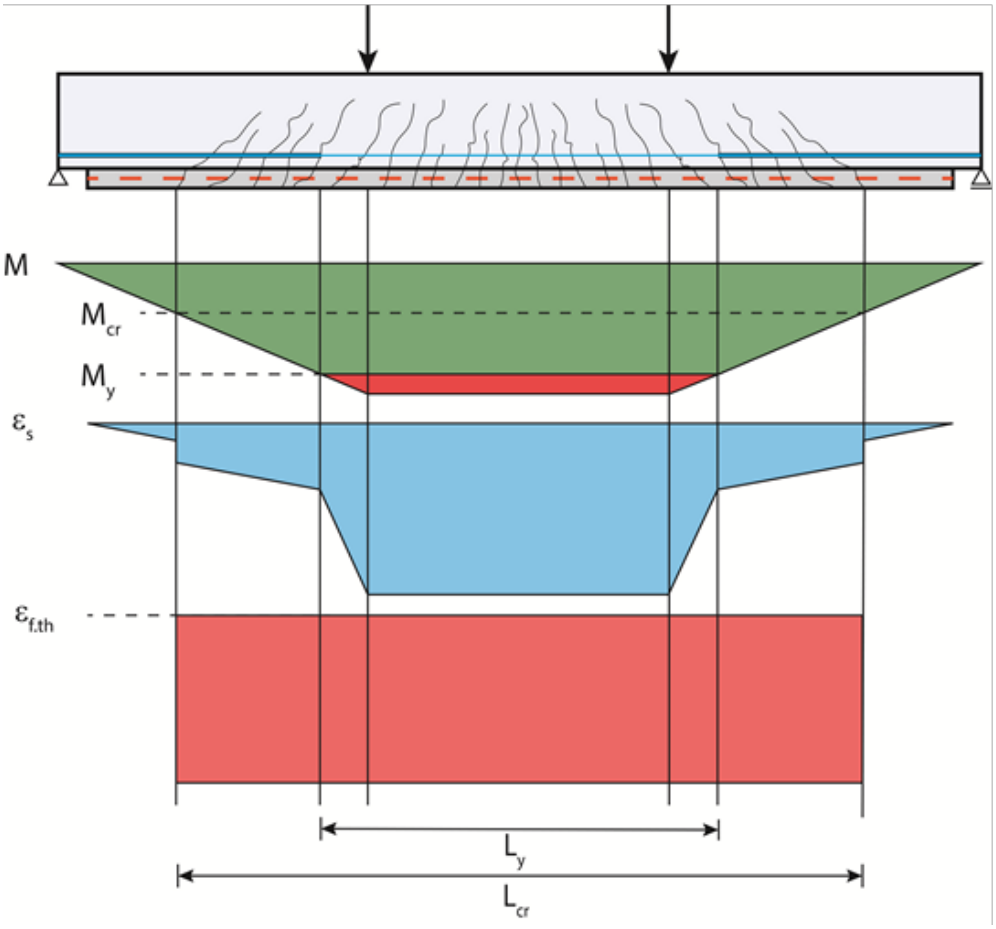

Figure 28 *Moment and strain distributions in unbonded approach considering cracked length*

To determine the strain in the steel reinforcement in the section with maximum bending moment, strain compatibility was used again, applying the same assumption of 3‰ maximum concrete strain. After finding sectional equilibrium, the theoretical bending moment is computed using the force in the textile that results from the previously computed strain and the force in the steel.

Comparing experimental to theoretical results returns an average M_{exp} / M_{theo} ratio greater than 1 (Figure 29), implying that this model underestimates the true bending capacity and thus, offers (overly) conservative results.

Only 20% of all experimental entries returned a M_{exp} / M_{theo} ratio lower than 1. The unbonded end-anchored approach underestimates the true bending capacity by 26% on average, with a COV of 24% (Table 9) again assuming normal distribution.

Table 9 *Statistics of unbonded approach considering cracked length*

	M_{exp}/M_{theo}
AVG	1.26
COV (ND)	24%

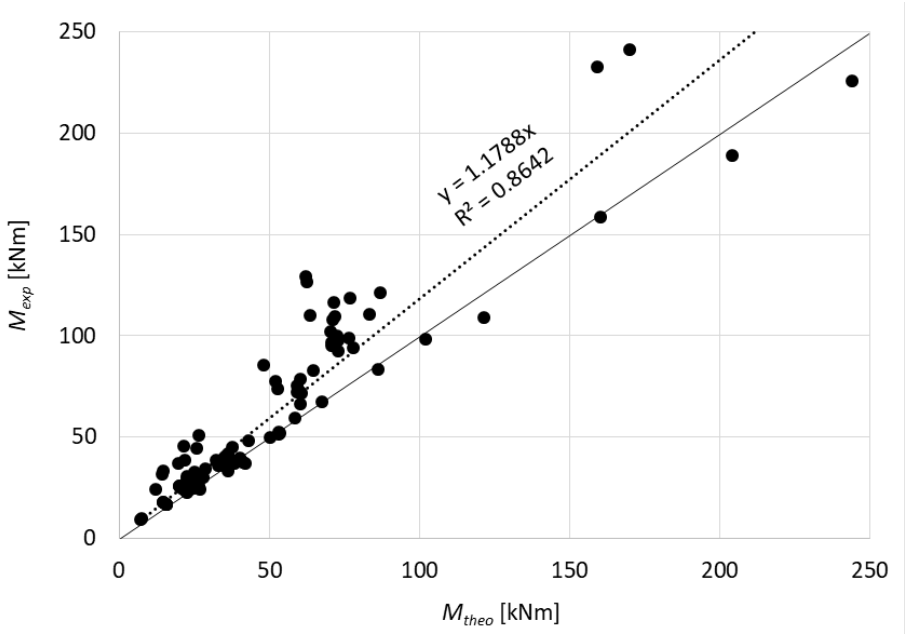

Figure 29 *Comparison of experimental and theoretical results for unbonded approach considering cracked length*

4.3.5 Length with yielding steel reinforcement

The effective length considered in computing the textile strain is the length on which the internal reinforcement is yielding. Based on the same principles as the previous one, this approach is can be regarded as another option of the unbonded approach.

By determining a weighted static height of textile and steel reinforcement, considering their axial stiffnesses, and applying usual analysis assumptions of elastically cracked reinforced concrete, the neutral axis position in the elastic state can be determined which allows to find the steel yielding moment and its position in the moment diagram, returning the length where the textile is considered to be activated (Figure 30).

Computing the strain in the textile from the deflection and the yielded length and using the yield force in the steel reinforcement, the theoretical bending capacity is determined and compared to the experimental data.

The results (Figure 31) show that this refined option of the unbonded, end-anchored approach still underestimates the real flexural capacity but by 12% on average only – thus, providing less conservative results overall – but with a somewhat higher COV of approx. 28% (Table 10).

Table 10 *Statistics of unbonded end-anchored approach considering yielding length*

	M_{exp}/M_{theo}
AVG	1.12
COV (ND)	28%

In this context, the test setup plays an important role: in 3-point bending, the yielding length is considerably reduced (Figure 32) in comparison to 4-point bending (Figure 30). However, the comparison of experimental and theoretical results does not provide a clear trend for this observation since the 3-point bending points are located on both sides of the diagonal, i.e. conservative and non-conservative, as for the 4-point bending results (Figure 31).

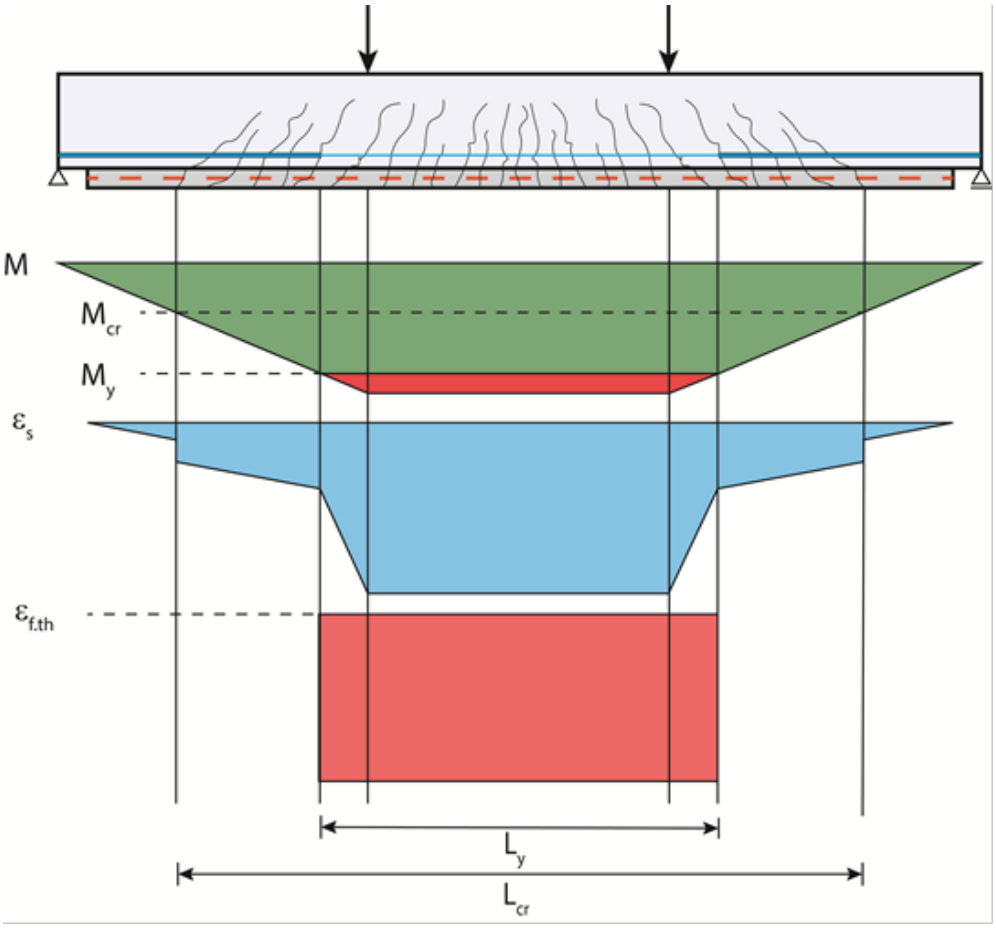

Figure 30 *Moment and strain distributions in unbonded approach considering yielding length*

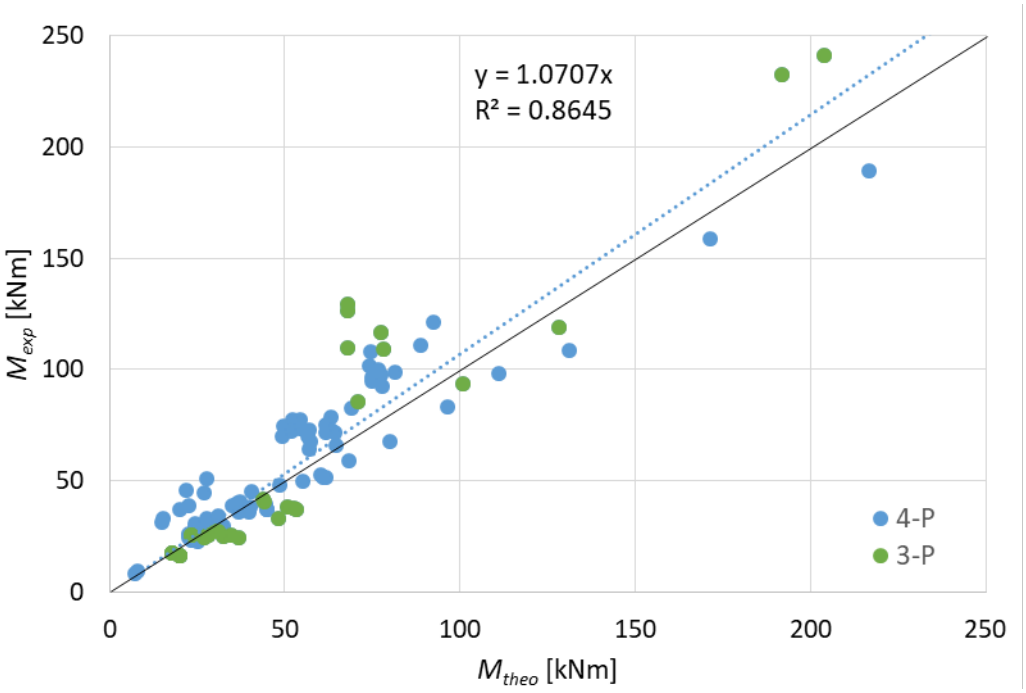

Figure 31 *Comparison of experimental and theoretical results for unbonded approach considering yielding length*

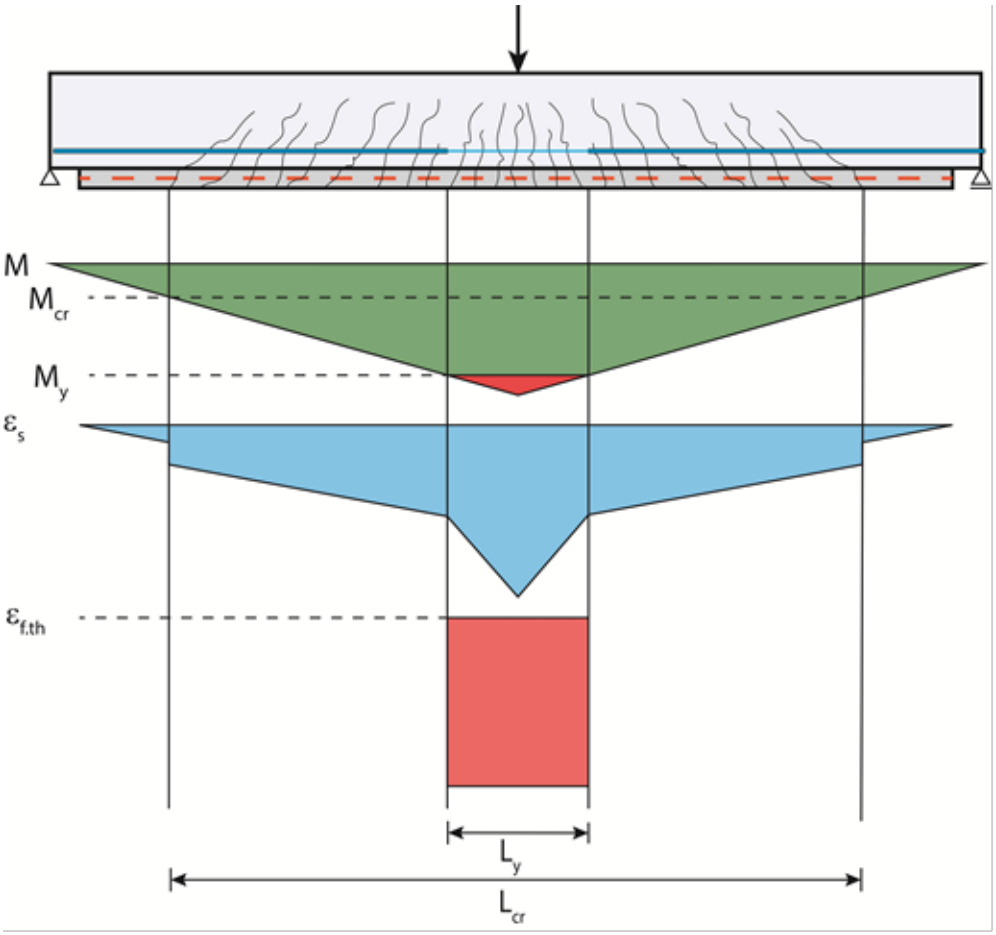

Figure 32 *Yielding length in 3-point bending*

4.3.6 Ultimate deflection in unbonded end-anchored approach

Overall, the unbonded end-anchored approach for the textile in combination with the steel yielding length returns considerably better results than the two previous ones (rigid bond or unbonded approach with cracked length, respectively). However, since the experimental deflection is used to compute the strain in the textile, it cannot be used as a dimensioning model because this parameter is unknown in practical situations.

So, it is evaluated what theoretical deflection must be used in the unbonded approach such that $M_{exp}/M_{theo} = 1$ is obtained for each of the database entries. Furthermore, a theoretically motivated expression is fitted using the previously determined deflections in order to obtain a ratio of $M_{exp}/M_{theo} = 1$ on average over all database entries.

The fitted expression (4.2) is similar to the deflection estimation expression of SIA 262 [34] which considers the textile reinforcement ratio ρ_t and the ratio between element height h and static height d, together with two fitting parameters c_1 and c_2:

$$\delta_M = \frac{C_1}{\rho_t^{c_2}} \left(\frac{h}{d}\right)^3 \delta_{th} \tag{4.2}$$

where $c_1 = 0.75$ and $c_2 = 0.75$,

and where

$$\delta_{th} = \frac{Pa}{24EI}(3L^2 - 4a^2) \text{ for 4-point bending} \tag{4.3}$$

$$\delta_{th} = \frac{PL^3}{48EI} \quad \text{for 3-point bending} \tag{4.4}$$

In Eq. (4.2), c_1 and c_2 are empirical values determined from curve fitting. In Eq. (4.3), a represents the shear span (i.e. distance from the support to the first point load).

The obtained theoretical deflections were used to compute the theoretical bending capacity which is compared to the experimental results (Figure 33 and Table 11).

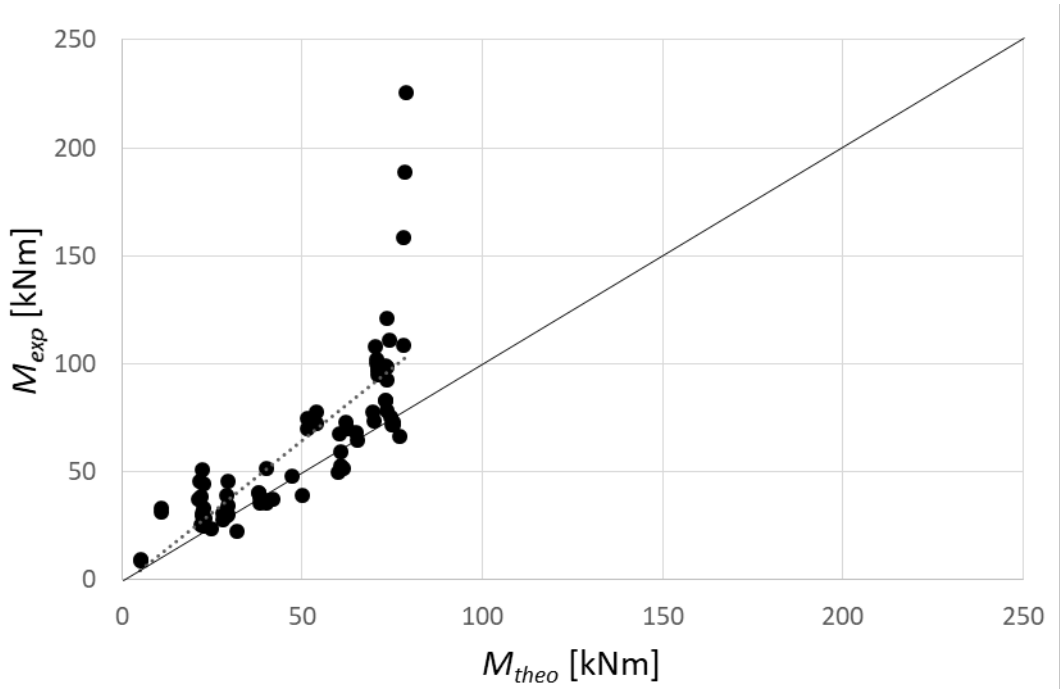

Figure 33 *Comparison of experimental and theoretical results for theoretical deflection approach*

Table 11 *Statistics of theoretical deflection approach*

	M_{exp}/M_{theo}
AVG	1.33
COV (ND)	36%

The results show that this approach based on ULS deflection results in overly conservative results, as the true bending capacity is underestimated by 33% on average and does not provide a considerably improved COV. In some cases, this approach returns extreme results as presented by the outliers in Figure 33, due to the averaging of the estimated deflections.

4.3.7 Friction coefficient approach

In this approach, which is similar to the previous one, instead of computing an average strain in the textile, a friction coefficient μ (Figure 34) between the textile and the mortar is considered on the cracked length such that $M_{exp}/M_{theo} = 1$ for every entry in the database.

The average value for the friction coefficient μ is 93.6 N/mm but the COV (ND) amounts to 152%. As such, this approach needs to be abandoned, too.

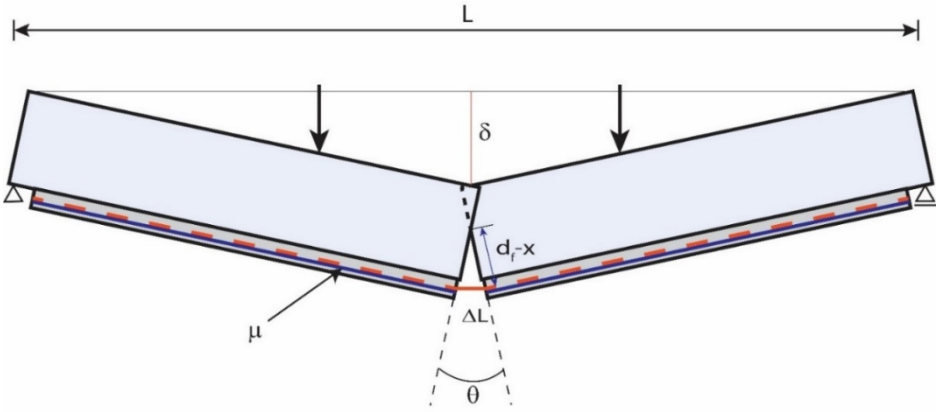

Figure 34 *Friction coefficient approach*

4.3.8 Bond coefficients approach

In this approach, the evaluation concentrated on the specimens were anchorage failure (i.e. slippage) was reported. The objective was to determine appropriate bond coefficients for steel and textile reinforcement, respectively, such that the ratio between the strain in the textile ($\varepsilon_{f,ex}$) at the first crack from the experiment – where the anchorage failure occurs – and the strain ($\varepsilon_{f,ma}$) determined from Maeder's approach (see 3.2) is one on average.

The bond coefficient of a reinforcement (steel or textile) represents the ratio k between the average strain (ε_{avg}) which results from strain compatibility and the maximum strain (ε_{max}) which is localized in the crack and is associated with the stress computed from sectional equilibrium.

The cracked length L_a and the cracking moment M_{cr} need to be determined in order to compute the efforts and strain in the textile at the first crack. This was done according to Eqs. (4.1) and (4.5). The experimental strain $\varepsilon_{f,ex}$ was computed by Eqs. (4.6) and (4.7).

$$M_{cr} = f_{ctm}\frac{I_y}{z_{max}} \tag{4.5}$$

$$\varepsilon_{f,ex} = \frac{M_{cr}}{\frac{EA_s}{k_s}\frac{(d_s - x_{cr})^2}{3(d_f - x_{cr})} + \frac{EA_f}{k_f}\frac{d_f - x_{cr}}{3}} \tag{4.6}$$

$$x_{cr} = \frac{\sqrt{2bE_{cm}\left(\frac{EA_s d_s}{k_s} + \frac{EA_f d_f}{k_f}\right) + \left(\frac{EA_s}{k_s} + \frac{EA_f}{k_f}\right)^2} - \left(\frac{EA_s}{k_s} + \frac{EA_f}{k_f}\right)}{bE_{cm}} \tag{4.7}$$

It can be seen that the textile strain also depends on the steel reinforcement bond coefficient k_s. Considering k_s to be between 0.5 and 0.65, as a function of steel reinforcement diameter, yield strength, crack spacing, and concrete strength as in the Tension cord model, results in textile bond coefficients of k_f = 0.69 for specimens strengthened with PBO and k_f = 0.88 for specimens strengthened with carbon, reflecting a ratio of 1 between the theoretical and experimental strain but also a high COV, Table 12.

Table 12 *Statistics of the bond coefficients approach*

	M_{exp}/M_{theo}
AVG	1.33
COV (LND)	36%

As this high COV is not satisfying either, this model together with all the previously described ones was discarded.

5 Proposal for flexural strengthening design of one-way slabs with TRC

5.1 Strain limit approach

Inspired by SIA 166 [35], the approach proposed here targets at identifying limits of the maximum strain in the textile reinforcement at ULS while the stress in the steel reinforcement is considered to be the tensile strength (Figure 35).

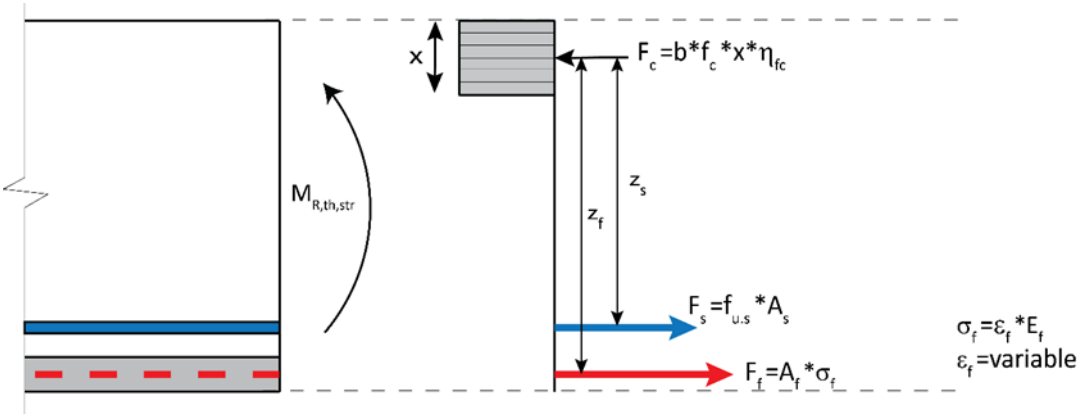

Figure 35 *Strain limit approach*

The assumption for the steel stress at failure is justified by evaluating the test results from unstrengthened specimens only, resulting in M_{exp} / M_{theo} = 1.0 on average and a COV of 15%.

In the compression zone, a simple stress block with a reduction coefficient according to [34] for the concrete compressive strength is considered. The assumption for the concrete stress distribution has an impact on the lever arm of tensile forces, in the first place (Figure 35), and does not undergo important variations after cracking.

With these assumptions, bending capacity can essentially be calculated from equilibrium only. Obviously, this approach is only applicable for slender slab elements with relatively low reinforcement ratios – which is normally the case for bridge deck slabs. For more general applications, i.e. for generic geometries of the cross-section and reinforcement ratios, the strain limit approach explored here cannot necessarily be applied.

In a first general step, a strain limit of $\varepsilon_{f,lim,u}$ = 6.6‰ is found considering all database entries, regardless of failure type or textile material, to obtain M_{exp} / M_{theo} = 1.0 on average and using the respective elastic modulus of the textile fibers (Table 1), i.e. efficiency coefficient η is implicitly contained in the derived strain limit. The associated COV is low (Table 13). Note that a log-normal distribution is considered here but the difference to the COV of a normal distribution (17.7%) is very small.

Table 13 *Statistics for general strain limit of $\varepsilon_{f,lim,u}$ = 6.6‰*

	M_{exp}/M_{theo}
AVG	1.00
COV (LND)	16.90%

Refining this approach in a second step, differentiated strain limits are derived for the strengthening textile materials (Table 14). With these strain limits, the COV for log-normal distribution is furthered lowered to 15.1% (15.8% for normal distribution) while maintaining M_{exp} / M_{theo} = 1.0 on average.

Table 14 *Strain limits per textile material*

Material	Carbon	PBO	Basalt	Glass
Strain limit [‰]	4.5	8.0	12.0	8.0

As shown in Figure 36, the consideration of these ultimate strain limits, as a function of the textile material, results in very good agreement between experimental and theoretical results while being a simple, practical and still conservative approach for the dimensioning of TRC strengthening layers of slender under-reinforced concrete slabs (i.e. reinforcement ratios low enough for attaining concrete crushing while the steel reinforcement yields).

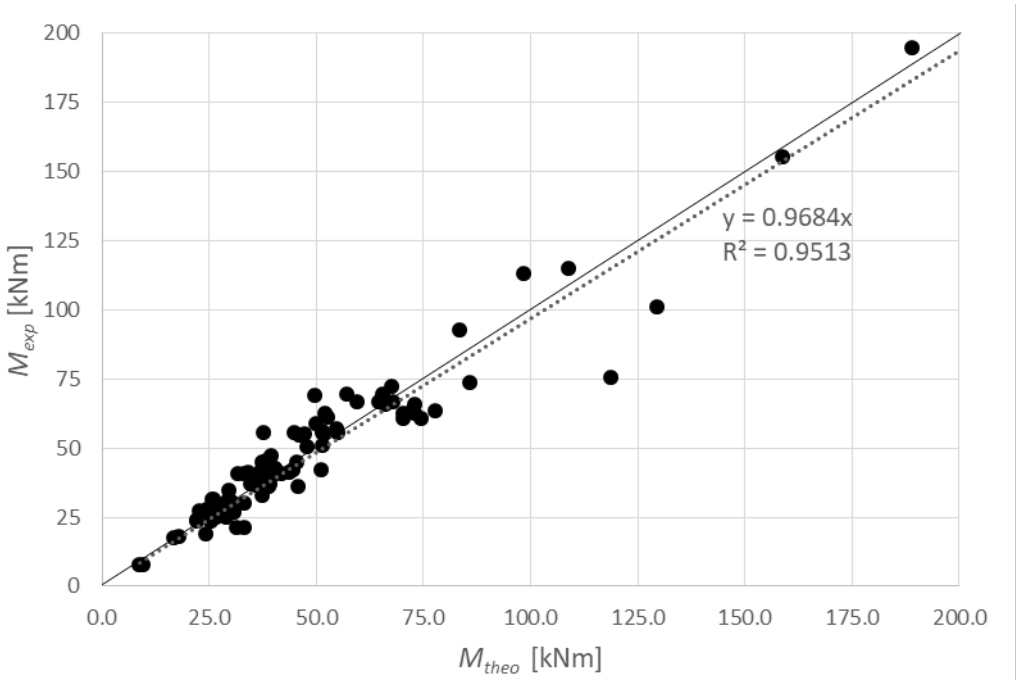

Figure 36 *Comparison of experimental and theoretical results for different strain limits per textile material*

In a further refinement step, differentiated strain limits for each failure type are derived per textile material (Table 15). These values do not differentiate for the number of textile layers while the available experimental data majorly covers specimens with up to four layers (Figure 23).

Table 15 *Strain limits per textile material and failure type*

Textile material	Carbon	PBO	Basalt	Glass
No. of test data	33	45	14	8
Failure type	Average strain [‰]			
Delamination	4.45	7.1	32.5	8.0
Slippage	4.50	9.2	7.05	18.0
Yarn rupture	4.90	-	32.5	8.0
Concrete crushing	-	9.2	-	-
Weighted AVG	4.55	7.90	12.50	10.5

The considered type of failure is the one reported for each experiment in the database. Slippage stands for anchorage failure of the fibers while delamination represents bond failure at the interface between the first textile layer (from the concrete support) and the mortar matrix. Concrete crushing happened in two cases only, and fiber rupture was attained only in twelve cases with glass and carbon fiber textiles (Table 7).

For PBO textiles, the most frequent failure type is delamination while for carbon and basalt it is slippage. Glass textile reinforced specimens mostly failed by fiber rupture. As the number of database entries with basalt and glass textiles is low, for statistical reasons, the strain limits of those materials are not recommended to be used.

Note again that the efficiency coefficient η is implicitly contained in the strain limits shown in Table 15. Comparing the yarn rupture strain limit of carbon and glass fiber textiles with their ultimate strain (Table 1) results in η-values of 0.25 and 0.27, respectively, confirming

the order of magnitude of values given in literature (Table 2). For the other textile failure types, i.e. delamination and slippage, the values of η cannot really be determined because the reference strain of the fibers is lower than the ultimate strain but a priori unknown. Still, if the derived strain limits are compared to the ultimate strain (Table 1), the associated efficiency coefficients result in 0.33 for PBO textile delamination and in 0.22 for basalt textile slippage, being in a comparable order of magnitude as the values reported in the literature (Table 2).

By applying the strain limits from Table 15, M_{exp}/M_{theo} = 1.0 is maintained while the COV is further reduced (Table 16) to a very low value, regarding the variability that must usually be expected when studying reinforced concrete elements.

***Table 16** Statistics for variable strain limits per material and failure type*

Material	Carbon	PBO	Basalt	Glass
COV (LND)	13.5%	11.5%	15.4%	8.9%
COV (ND)	14.6%	11.8%	15.4%	9.1%

Figure 37 shows theoretical to experimental ultimate bending capacities, considering strain limits per material and failure type. It becomes evident that this approach (among those investigated) offers the best results for dimensioning flexural strengthening with TRC of slender reinforced concrete slabs with rather low reinforcement ratios.

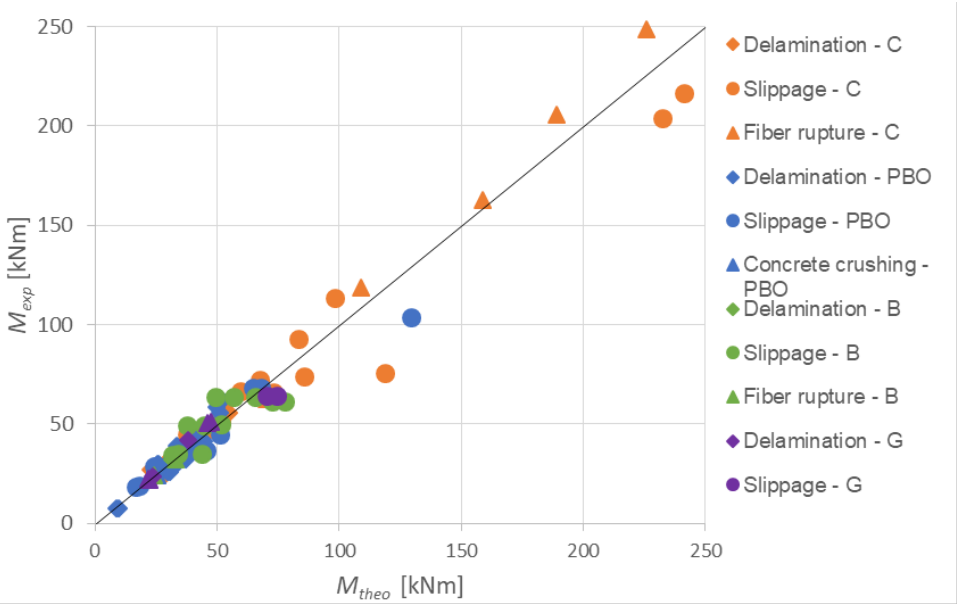

***Figure 37** Comparison of experimental and theoretical results for variable strain limits per material and failure type*

5.2 Structural analysis and dimensioning

The objective of this research is to determine an analytical model that can be used for dimensioning of the strengthened bridge deck slabs. Since the analytical model is based on limit strains, the proposed design method considers the lowest strains that account for various failure mechanisms, regardless of the location in which they are taking place. For Carbon and PBO fibers, it results that delamination failure is prone to happen on average at a lower strain than slippage failure.

5.2.1 Sectional analysis

When the flexural capacity of existing bridge deck slabs according to SIA 262 [34] does not satisfy the ULS requirements of SIA 260 [36], one option is to refine structural analysis

results (for example, according to the procedures suggested in [37]), update mechanical properties intervening on the flexural capacity of the existing deck slab in more depth (that is, the reinforcement ratio and its mechanical quality, above all), and to consider reduced loads according to SIA 269/1 [38]. If all these refinements do not lead to a satisfying result, flexural strengthening is required.

For dimensioning the flexural capacity of the strengthened slab element, it is suggested to use Eqs. (5.1) to (5.7) as presented in Figure 38. This design approach conservatively considers the design yield strength f_{sd} as the maximum stress in the steel reinforcement. This intentionally differs from what is shown in 5.1, where the theoretical results were well correlated with the experimental ones considering the tensile strength of the steel.

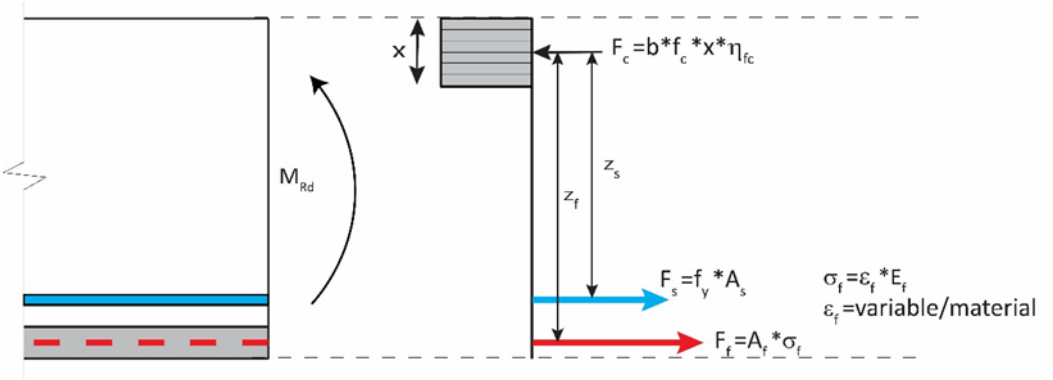

Figure 38 *Flexural design approach*

If Eq. (5.7) is not satisfied with a first textile layer, another layer should be added which also changes the effective depth of the textile strengthening. In this context, one should pay attention to the fact that the textile reinforcement effectiveness starts to be reduced if more than four layers are applied. The flexural capacity increase provided by TRC can reach 20-25% per applied textile layer (for up to four layers) as the empirical evaluation of experimental data for slab and beam specimens showed (see 4.2). If this number of textile layers is not enough to increase the flexural capacity to a satisfactory level, other strengthening methods should be evaluated as options.

$$M_{Rd} = A_s f_{sd} z_s + A_f E_f \varepsilon_{fd} z_f \tag{5.1}$$

where ε_{fd} is the design strain of the textile (see 5.2.2), and E_f is the elastic modulus of the textile yarn material (Table 1)

$$F_c = F_f + F_s \tag{5.2}$$

$$F_f = A_f E_f \varepsilon_{fd} \tag{5.3}$$

$$F_s = A_s f_{sd} \tag{5.4}$$

$$F_c = 0.85 x b f_{cd} \tag{5.5}$$

$$z_i = d_i - \frac{0.85x}{2} \tag{5.6}$$

$$M_{Rd} \geq M_{Ed} \tag{5.7}$$

5.2.2 Characteristic and design values

The basic input for determining the textile design strain ε_{fd} is the characteristic strain at failure. According to [39], the required characteristic textile strength ($f_{f,k}$) can be estimated as the average value minus 2.33 times the standard deviation – thus, referring to the 1st percentile of a normal distribution. It may be presumed, however, that this value rather refers to the textile strength itself – which varies quite little when tested correctly [9] – but not necessarily to the failure strain of a yarn bonded to the surrounding cementitious matrix.

Hence, to shift from average values of strain limits (Table 15) to characteristic strains, the approach proposed by SIA 269/2 [40] for steel reinforcement for a sample size between 3 and 30 elements is applied (which considers a normal distribution):

$$\varepsilon_{f,k} = \varepsilon_{fm}(n) - k_5(n)s \tag{5.8}$$

$$k_5(n) = 1.28 + 5n^{-4/5} \tag{5.9}$$

where $3 \leq n \leq 30$ is the number of samples and s is the standard deviation.

Table 17 summarizes the derived characteristic strains per textile material and failure type and shows the considered input values. As done for the average values, no differentiation in limit strain is made for the number of textile layers; still, note again that the database majorly contains results for specimens with up to four textile layers.

Table 17 *Characteristic strain limits for up to four textile layers*

Yarn material	Failure type	ε_{fm} [‰]	*s (ND)*	*n*	k_5	$\varepsilon_{f,k}$ [‰]
Carbon	Delamination	**4.45**	0.10	12	1.96	4.26
	Slippage	4.5	0.19	15	1.85	**4.15**
	Yarn rupture	4.9	0.11	6	2.47	4.62
PBO	Delamination	**7.1**	0.12	28	1.63	**6.91**
	Slippage	9.2	0.13	15	1.85	8.97
	Concrete crushing	9.2	0.07	2	-	-
Basalt	Delamination	32.5	-	1	-	-
	Slippage	**7.05**	0.17	11	2.01	**6.70**
	Yarn rupture	32.5	0.02	2	-	-
Glass	Delamination	8	0.06	2	-	-
	Slippage	18	0.05	2	-	-
	Yarn rupture	8	0.05	4	2.93	7.85

For carbon textiles, it can be observed that the lowest average strain for delamination failure does not result in the lowest characteristic strain. This is obviously due to the differences in standard deviation (*s*) and number of test results (*n*). For structural design purposes, however, the smallest characteristic strain should be considered, i.e. slippage failure, even if this failure type may not necessarily be governing at attaining the real ultimate capacity associated to average material properties. However, the difference in characteristic strains for the two priority failure types, i.e. delamination and slippage, is quite small and thus, this differentiation is more academic than of practical relevance.

For PBO fiber textiles, the number of test results where concrete crushing would occur is too low to derive characteristic values. As this type of failure is not directly associated to the material used for strengthening the tension zone, it is of little importance in the present case. Yarn rupture was not observed in the tests (Table 7).

For basalt fiber textiles, the number of test results where delamination or yarn rupture would occur is too low to derive characteristic values. The number of test results for slippage failure may be sufficiently high but some prudence should be used as this may not be the only failure type for this textile material.

For glass fiber textiles, the number of samples is also too low to derive characteristic strains for delamination and slippage failure. The number of samples is just high enough for yarn rupture which seems to be one of the possibly governing failure types when looking at the average failure strains (Table 15) and at the experimentally observed failures (Table 7).

In order to use these characteristic strain limits in practical structural design, they need to be corrected with partial safety and conversion coefficients η_f and γ_M as requires Eq.(5.10):

$$\varepsilon_{fd} = \frac{\eta_f \varepsilon_{f,k}}{\gamma_M} \tag{5.10}$$

A material safety factor of γ_M = 1.3 for tensile strength, together with a durability safety factor α as a function of the material, is recommended by Curbach et al. [41] to determine the design value f_{fd}, Eq. (5.11):

$$f_{fd} = \frac{f_{f,k}}{\gamma_M \alpha} \tag{5.11}$$

where γ_M = 1.3 and α = 2.44 for glass fibers and α = 1.18 for carbon fibers. The α-values correspond to the inverse of η according SIA 260 [36] and amount to η_f = 0.41 and η_f = 0.85 for glass and carbon fibers, respectively.

Just [42] recommends using a material safety factor of γ_M = 1.2, together with further coefficients which account for temperature influence, expected lifetime and durability, Eq. (5.12):

$$f_{fd} = \alpha_{T,t} \alpha_{t\infty,t} \alpha_{D,t} \frac{f_{f,k}}{\gamma_M} \tag{5.12}$$

where $\alpha_{T,t}$= 0.85, $\alpha_{t\infty,t}$= 0.7 and $\alpha_{D,t}$= 0.7. This results in a total reduction comparable to Eq. (5.11) for glass fibers, i.e. η_f = 0.42.

Rempel et al. [43] look at required partial safety factors of very thin flexural elements made of textile reinforced concrete only. The also suggest a material safety factor of γ_M = 1.3 and found out that the necessary safety factor is primarily influenced by the static height of the textile and its geometrical reinforcement ratio. Among the negligible influences also figures the reduction coefficient for sustained loading which is assumed to be 0.6 for glass fiber textiles and 0.9 for carbon fiber textiles, respectively. As such, they conclude that the proposed partial safety factors are generally applicable for resin saturated textiles.

From the available research results on partial safety factors and reduction coefficients, it becomes clear that final recommendations cannot be provided here, in particular not for basalt fiber textiles. For the often applied carbon fiber textiles, a conservative assumption seems to be the proposal shown in Eq. (5.11) and the associated values.

Furthermore, the anchorage capacity of the textile should be verified, for the anchorage of the textile beyond the first theoretical crack which can be derived in analogy to SIA 166 [35]. The anchorage capacity can be computed using the method proposed by Maeder [18], see 3.2. The anchorage length should be considered as in 4.3.3, outside of the cracked length. This length can be computed starting from the moment capacity at midspan M_{Rd} and using the tensile strength of the mortar (which could possibly be adapted to satisfy the needed anchorage length).

6 Conclusion

Textile reinforced concrete TRC (also known as textile reinforced mortars or fabric reinforced cementitious matrix, respectively) represents a solid alternative for flexural strengthening of existing reinforced concrete elements, especially for two-dimensional elements like one-way slabs. The main advantages of using this system are easy mounting and good fire resistance compared to externally bonded reinforcements with fiber reinforced polymers.

The flexural capacity increase provided by TRC can reach 20-25% per applied textile layer (for up to four layers) as the empirical evaluation of experimental data for slab and beam specimens showed. For a stringent dimensioning in practice, however, experimentally verified theoretical approaches are required – the main objective of this study. Starting from principles and methods for reinforced concrete, a first approach considering rigid bond between textile and mortar (as it is regularly performed for steel reinforcement, too) proved to considerably overestimate the real flexural capacity of strengthened specimens and furthermore, with a high coefficient of variation COV. Based on this result, it becomes clear that axial stiffness efficiency coefficients for the textile (resulting from particularities of these textile yarns w.r.t. internal bond and to the surrounding mortar matrix), as also promoted in literature, have to be introduced. With the values proposed in literature, however, a clear underestimation of the true flexural capacity results, but with a somewhat reduced COV.

As such, one could be tempted to consider these textiles like an unbonded end-anchored reinforcement, as done for unbonded prestressing. The force increase in the reinforcement can then be calculated with a rigid body failure mechanism but also requires a reference length between anchorages to determine the textile force increase. In a first step, it is intuitive to consider the cracked length of the TRC while the textile ends are anchored in the uncracked zones. Such an approach results in very conservative estimations of flexural capacity but also a further reduced COV. The next step was to reduce the unbonded length to the length on which the internal steel reinforcement is yielding. This approach rendered clearly better results on average, yet the main setback was with 3-point bending specimens where this length could not be reasonably determined.

Starting from the previous attempt and considering proposals from literature for externally bonded reinforcement EBR, another approach was applied considering different bond coefficients for the textile and for the internal steel reinforcement. A set of bond coefficients could be determined to have analytical results comparable to experimental values, yet the very high COV rendered this approach unsatisfactory, too. The analytical model presented in 5.1 also refers to approaches for EBR as it identifies strain limits for the textile as a function of the textile material and the (experimentally observed) failure type. It proved to be the most reliable approach given its accuracy in comparison to the experimental data and its very low COVs. A drawback is that this approach does not explicitly consider where exactly the textile fails, as it simply limits the textile strain associated to the maximum bending moment, as if it was fiber rupture at the cross-section with maximum bending. However, slippage and delamination failures occur more often, where slippage stands for textile anchorage failure while delamination refers to bond failure at the interface between the first textile layer (from the concrete support) and the mortar matrix. These failures would rather happen in zones with higher shear forces or close to the supports, respectively.

But, the proposed design approach for flexural strengthening has the advantage of being practice-oriented since it uses usual dimensioning principles in a generally accepted way. If the strain limit approach is complemented with the verification of the textile's anchorage capacity behind the first theoretical crack (analogously to SIA 166 [35]), an adequately conservative dimensioning should be possible. A dimensioning approach for the anchorage capacity of textiles embedded in mortar, based on a theoretical bond-slip constitutive law proposed in literature for single textile yarns as well as on experimental data from own and published tests, is presented in 3.2. The proposed dimensioning approach shows accurate agreement with experimental results and satisfactory COVs. It further provides evidence that the maximum anchorage capacity is capped for long anchorage lengths (due to limited bond rupture energy), and it will usually not reach the capacity of the textile yarns.

7 Further research needs and practical implication

To further develop practical applications of textile reinforced concrete (TRC) strengthening for slab elements, additional experimental studies that focus on impacts of multiple textile layers should be conducted, in particular three and more textile layers, to determine their effectiveness. This should be done, on the one hand, by experimentally identifying the anchorage capacity of multiple textile layers for variable anchorage length. To eliminate tolerance impacts in specimen and test setup fabrication, it is recommended to use single lap push-pull test setups. On the other hand, experimental data on full-scale (or real-scale, at least) flexural specimens is required as a basis of comparison to analytical approaches. In the latter experimental studies, a further focus should be set on reproducing realistic loading schemes, i.e. four- or even asymmetric six-point loading to simulate the effects of usually governing wheel load schemes on bridge deck slabs.

In theoretical evaluations, particular attention should be paid to the derivation of efficiency factors of textiles, i.e. their rupture stress in comparison to the failure stress of the pure textile fiber. These efficiency factors also go together with the bond behavior of embedded textile yarns. Thus, further experimental and, above all, theoretical investigations on the influence of the bond behavior between textile and surrounding mortar over the whole length of a flexurally strengthened slab element should be conducted, in order to derive an analytical model for tension stiffening effects in TRC that is able to replicate experimental results with high accuracy and reliability. A useful basis for such analytical investigations is provided by Maeder's bond model, developed for the anchorage capacity of TRC (3.2.6), that can be extended to evaluating the structural behavior of tension chords made of textile reinforced concrete and their impact on the structural behavior of strengthened reinforced concrete slabs. As shown in preliminary evaluations by this model, the tension stiffening effects in TRC may possibly be modelled by a three-stepped perfectly plastic bond behavior which requires, in the first place, the determination of associated tensile stress or strain limits for regime changes in the bond behavior. In these derivations, the TRC geometry (i.e. ratio of gross textile area to mortar area, efficiency factors, and yarn bond perimeter, above all) should play essential roles.

The suitability of the proposed limit strain approach could be further investigated and verified by full-scale test results, in particular for basalt and PBO textiles. The approach could also be extended to more general situations (high steel reinforcement ratio, more variable ratios of member to static height etc.). These investigations should be combined with clear identification of governing control sections for structural dimensioning of TRC strengthening. Furthermore, normative guidelines (SIA) should be made available. These require the consideration of conversion and material safety factors, as well as characteristic values for strain limits. While the latter can principally be deduced from the results provided here, the former are a priori unknown. Section 5.2.2 provides some information from literature for these material safety factors and conversion coefficients but nationally applicable values should be derived. Furthermore, there is definitely a need for including normative guidelines for textile reinforced concrete in Swiss codes, for example in a revision of SIA 166 (which is already more than 15 years old, anyway).

Due to the lack of sufficiently comprehensive experimental data in literature, the effects of flexural strengthening on the shear capacity of concrete slab elements (that is, elements without shear reinforcement) could not be investigated here. Such investigations can go together with the experimental and theoretical evaluation of tension stiffening effects provided by the flexural strengthening and they, in turn, will be related again to the bond behavior between textile and surrounding mortar. Similarly, improvements of fatigue resistance and serviceability behavior of existing reinforced concrete bridge deck slabs by applying TRC strengthening represent other points of interest that need to be investigated, coming along with investigations on bond degradation due to reversed cyclic textile loading from fatigue loads, which has not been part of the research presented in this report.

Glossary

Symbol / acronym	Explanation
TRC	Textile reinforce concrete
FRCM	Fabric reinforced cementitious matrix
PBO	Poly-phenylene-2,6-benzobisoxazole
B	Basalt fiber
C	Carbon fiber
G	Glass fiber
ULS	Ultimate state limit
COV	Coefficient of variation
3 / 4 PB	3 / 4 point bending test setup
D,d	Diameter
E_f	Young's modulus for textile fibers
A_f	Cross section area
$f_{f.u}$	Textile ultimate strength
$\varepsilon_{f.u}$	Textile ultimate strain
$f_{f.k}$	Textile characteristic strength
$\varepsilon_{f.k}$	Textile characteristic strain
$f_{f.d}$	Textile design strength
$\varepsilon_{f.d}$	Textile design strain
γ_M	Partial safety factor
η	Reduction coefficient, bond efficiency coefficient
α	Reduction factor
S	Slip, standard deviation
τ_{max}	Bond stress
ψ	Circumference
κ	Elastic bond stiffness
P	Pullout force / Load
C	Constant
Z, z	Lever arm
D	Static height
x	Compression height
$M_{exp,/th}$	Experimental/theoretical bending moment
ΔL	Elongation
δ	Deflection
θ	Rotation
L_{cr}	Cracked length
L_y	Yielding length
L_a	Anchorage length
L	Length, span

b	Width
H	Height
a	Distance from the support to first point load
μ	Friction coefficient
k	Reduction factor
n	Number of specimens

References

[1]	https://en.wikipedia.org/wiki/Textile-reinforced_concrete#cite_note-:3-1
[2]	https://zoltek.com/carbon-fiber/how-is-carbon-fiber-made/
[3]	Williams Portal N., Lundgren K., Wallbaum H. and Malaga K. (2014). “Sustainable Potential of Textile-Reinforced Concrete”. Journal of Materials in Civil Engineering, 27(7), DOI: 10.1061/(ASCE)MT.1943-5533.0001160.
[4]	Fernández M. and Muttoni A. (2017). Building in a lighter and more sustainable manner: textile reinforced concrete for thin structural elements. Cemsuisse, project nr. 201407.
[5]	Jung K., Hong K., Han S., Park J. and Kim J. (2015). “Prediction of flexural capacity of RC beams strengthened in flexure with FRP fabric and cementitious matrix”. International Journal of Polymer Science, Article ID 868541.
[6]	Ombres L. (2011). “Flexural analysis of reinforced concrete beams strengthened with cement based high strength composite material”. Composite Structures Journal, 94:143-155.
[7]	Li J. and Zhao Z. (2009). “Study on Mechanical Properties of Basalt Fiber Reinforced Concrete”. Materials Science and Engineering A, 505(1):178-186.
[8]	Al-Lami K., D’Antino T. and Colombi P. (2020). “Durability of Fabric-Reinforced Cementitious Matrix (FRCM) Composites: A Review”. Applied Sciences, 10(5):1714-1737.
[9]	Michels J., Zwicky D., Scherer J., Harmanci Y.E. and Motavalli M. (2014). “Structural Strengthening of Concrete with Fiber Reinforced Cementitious Matrix (FRCM) at Ambient and Elevated Temperature – Recent Investigations in Switzerland“. Advances in Structural Engineering, 17(12):1785-1799.
[10]	Maeder M. (2017). Grid anchorage in textile reinforced concrete – State of the art. Master project report, School of Engineering and Architecture of Fribourg (HEIA-FR).
[11]	EN 1992-1-1 (2004). Eurocode 2: Design of concrete structures - Part 1-1: General rules and rules for buildings. Brussels: European committee for standardization.
[12]	Brameshuber W. (2016). “Recommendation of RILEM TC 232-TDT: test methods and design of textile reinforced concrete”. Materials and structures, 49(12):4923-4927.
[13]	Schütze E., Bielak J., Scheerer S., Hegger J. and Curbach M. (2018). ”Einaxialer Zugversuch für Carbonbeton mit textiler Bewehrung“. Beton- und Stahlbetonbau, 113(1):33-47.
[14]	Maeder M. (2017). Grid anchorage in textile reinforced concrete – Parametric study and experimental program proposal. Master project report, School of Engineering and Architecture of Fribourg (HEIA-FR).
[15]	Mobasher B. (2012). Mechanics of Fiber and Textile Reinforced Cement Composites. Boca Raton: CRC Press.
[16]	Ulaga T. (2003). Betonbauteile mit Stab- und Lamellenbewehrung: Verbund- und Zuggliedmodellierung. Dissertation Nr. 15062, Institut für Baustatik und Konstruktion (IBK), Eidg. Technische Hochschule (ETH), Zürich.
[17]	Richter M. (2005). Entwicklung mechanischer Modelle zur analytischen Beschreibung der Materialeigenschaften von textilbewehrtem Feinbeton. Berichte des Instituts für Mechanik und Flächentragwerke, Heft 2, Dresden.
[18]	Maeder M. (2018). Grid anchorage in textile reinforced concrete – Experimental and analytical development of a structural design model. Master thesis report, School of Engineering and Architecture of Fribourg (HEIA-FR).
[19]	https://www.sp-reinforcement.ch/de-CH/produkte
[20]	Loreto G., Leardini L., Arboleda D. and Nanni A. (2014). “Performance of RC slab-type elements strengthened with fabric reinforced cementitious matrix composites”. Journal of Composites for Construction, 18(3), DOI: 10.1061/(ASCE)CC.1943-5614.0000415.
[21]	Babaeidarabad S., Loreto G. and Nanni A. (2014). “Flexural strengthening of RC beams with externally-bonded fabric reinforced cementitious matrix (FRCM)”. Journal of Composites for Construction 18(5), DOI: 10.1061/(ASCE)CC.1943-5614.0000473.
[22]	D’Ambrisi A. and Focacci F. (2011). “Flexural strengthening of RC beams with cement-based composites”. Journal of Composites for Construction, 15(5), DOI: 10.1061/(ASCE)CC.1943-5614.0000218.
[23]	Ebead U., Shrestha K., Afzal M., Refai A. and Nanni A. (2017). “Effectiveness of fabric reinforced cementitious matrix in strengthening reinforced concrete beams”. Journal of Composites for Construction, 21(2), DOI: 10.1061/(ASCE)CC.1943-5614.0000741.

[24]	Schladitz F., Frenzel M., Ehlig D. and Curbach M., (2012). “Bending load capacity of reinforced concrete slabs strengthened with textile reinforced concrete”. Engineering Structures, 40:317-326.
[25]	Bisby L. and Stratford T. (2009). “Fiber reinforced cementitious matrix systems for fire-safe flexural strengthening of concrete: Pilot testing at ambient temperatures”. In: Advanced Composites in Construction, Birmingham.
[26]	Jabr A., El-Ragaby A. and Ghrib F. (2017). “Effect of the fiber type and axial stiffness of FRCM on the flexural strengthening of RC beams”. Fibers Journal, 5(1):2.
[27]	Elghazy M., Refai A., Ebead U. and Nanni A. (2016). “Performance of corrosion-aged reinforced concrete (RC) beams rehabilitated with fabric reinforced cementitious matrix (FRCM)”. In: 4th International Conference on Sustainable Construction Materials and Technologies, Las Vegas.
[28]	Elsanadedy H., Almusallam T., Alsayed S. and Al-Salloum Y. (2013). “Flexural strengthening of RC beams using reinforced mortar – Experimental and numerical study”. Composite Structures, 97:40-55.
[29]	Zwicky D. (2013). “Concrete slab strengthening with CFRP textile reinforced shotcrete”. In: IABSE Symposium 'Assessment, Upgrading and Refurbishment of Infrastructures’, Rotterdam.
[30]	Herbrand M., Adam V., Classen M., Kueres D. and Hegger J. (2017). “Strengthening of existing bridge structures for shear and bending with carbon textile-reinforced mortar”. Materials Journal, 10(9):1099.
[31]	Escrig C., Gil L. and Bernat-Maso E. (2017). “Experimental comparison of reinforced concrete beams strengthened against bending with different types of cementitious matrix composite materials”. Construction and building materials, 137:317-329.
[32]	Lee S., Hong K., Yeon Y. and Jung K. (2018). “Flexural Behavior of RC Slabs Strengthened in Flexure with Basalt Fabric-Reinforced Cementitious Matrix”. Advances in Materials Science and Engineering, Art. ID 2982784.
[33]	Ebead U. and El-Sherif H. (2019). “Near surface embedded-FRCM for flexural strengthening of reinforced concrete beams”. Construction and building materials, 204:166-176.
[34]	SIA 262 (2013). Betonbau (Concrete structures). Zurich: Swiss Society of Engineers and Architects SIA.
[35]	SIA 166 (2004). Klebebewehrung (Externally bonded reinforcement). Zurich: SIA.
[36]	SIA 260 (2013). Basis of structural design. Zurich: SIA.
[37]	Fernández M., Rodrigues R. and Muttoni A. (2009). Dimensionnement et vérification des dalles de roulement des ponts routiers. Office fédéral des routes, rapport no. 636.
[38]	SIA 269/1 (2011). Existing structures – Actions. Zurich: SIA.
[39]	Ascione L., de Felice G. and De Santis S. (2015). “A qualification method for externally bonded Fibre Reinforced Cementitious Matrix (FRCM) strengthening systems“. Composites Part B, 78:497-506.
[40]	SIA 269/2 (2011). Existing structures – Concrete structures. Zurich: SIA.
[41]	Curbach M. and Schütze E. (2016). Entwicklung von Bemessungs- und Sicherheitskonzepten sowie standardisierter Prüfkonzepte zur Materialcharakterisierung von Carbonbeton. Basisvorhaben B3 – Teilvorhaben C3-B3-I-a: Abschlussbericht. Dresden: TU Dresden, Institut für Massivbau.
[42]	Just, M. (2015). “Sicherheitskonzept für Textilbeton“. Beton- und Stahlbetonbau Spezial Januar – Verstärken mit Textilbeton, Supplement 1, 42-46.
[43]	Rempel S., Ricker M. and Hegger J. (2020). “Zuverlässigkeitsanalyse für biegebeanspruchte Textilbetonbauteile – Ermittlung von Teilsicherheitsbeiwerten”. Beton- und Stahlbetonbau, 115(9):697-709.

Project closure

Schweizerische Eidgenossenschaft
Confédération suisse
Confederazione Svizzera
Confederaziun svizra

Eidgenössisches Departement für
Umwelt, Verkehr, Energie und Kommunikation UVEK
Bundesamt für Strassen ASTRA

FORSCHUNG IM STRASSENWESEN DES UVEK

Version vom 09.10.2013

Formular Nr. 3: Projektabschluss

erstellt / geändert am:	23.03.2021

Grunddaten

Projekt-Nr.:	AGB 2015/005
Projekttitel:	Strengthening of bridge deck slabs with textile reinforced concrete
Enddatum:	30.06.2021

Texte

Zusammenfassung der Projektresultate:

The report presents the suitability evaluation of various theoretical approaches for the structural design of the flexural strengthening of bridge deck slabs with textile reinforced concrete (TRC) at ultimate limit state (ULS). TRC is a composite material which combines the high tensile strengths of the fiber textiles with the bond capacity and the mechanical and thermal protection provided by fine-grained concrete (i.e. cement-based mortars). Besides being used in manufacturing of new TRC elements, these materials can also be used as strengthening solutions for existing reinforced concrete (RC) elements. The most frequently used textiles in this type of applications, usually applied in the form of meshes, are made from Carbon, Basalt, Glass and PBO (poly-phenylene-2,6-benzobisoxazole, also known as Zylon) fibers.
The mortar plays an important structural role as anchorage and bond agent for the textile yarns, besides offering an additional protection layer to the steel reinforcement of the existing RC element. A good preparation of the support surface is essential : it has to be roughened by hydro-demolition before applying the strengthening system in order to ensure a monolithic behavior at the interface.
The anchorage by bond was studied through an experimental campaign, complementing existing experimental data from the literature and allowing to calibrate a series of parameters of the theoretical model proposed in the literature. The study concluded with an analytical proposal for determining the bond anchorage capacity of the textile yarns embedded in mortar, described in the report.
To identify a suitable theoretical approach for dimensioning the flexural strengthening of existing one-way slab elements, a database with experimental results was created by gathering data from the literature. This database contains data from approximatively 150 experiments on strengthened and unstrengthened reference elements. Each entry describes 58 different parameters covering input data such as test setup, cross-sectional geometry, material properties and experimental failure loads. In a first step, the collected data was evaluated empirically to determine the type of textile materials used, the types of observed failure and increases in flexural capacity. The flexural capacity increase provided by TRC reaches 20-25% per applied textile layer (for up to four layers).
In a second step, different theoretical approaches for ULS design of the flexural strengthening with TRC were applied to evaluate their suitability by comparing the theoretical flexural capacity with the experimental results. A first approach considers rigid bond between textile and surrounding concrete matrix and results in a large overestimation of the flexural capacity. The second approach goes into the other extreme, considering no bond between textile and matrix but end-anchorages of the textile being provided by the mortar. This approach returns conservative estimations of the flexural capacity, yet it is not satisfactory due to a high coefficient of variation (COV). The third and fourth approaches evaluate the consideration of friction and bond coefficients, respectively, between textile and surrounding matrix. However, due to their inapplicability to 3-point bending configurations and high COVs, they were also considered unsatisfactory. Finally, an analytical method is retained that introduces strain limits for the textiles as a function of material and failure type while the existing steel reinforcement is considered to be yielding, in analogy to externally bonded reinforcement. Thanks to thoughtful calibration of the strain limits, this approach shows very good agreement with experimental results, providing an average of 1 for the ratio between experimental results and theoretical predictions and the lowest COV of all evaluated approaches. Practically applicable strain limits can be recommended for carbon and PBO fiber textiles only, as too few experimental data is available for textiles made of glass and basalt fibers.
Textile reinforced concrete represents a viable method for strengthening existing reinforced concrete elements in bending, especially for surface elements like one-way slabs. The main advantages are the ease of application which involves tools that are already in use on the construction site and better fire resistance (i.e. construction site robustness) compared to adhesively bonded solutions with fiber-reinforced polymers.

Schweizerische Eidgenossenschaft
Confédération suisse
Confederazione Svizzera
Confederaziun svizra

Eidgenössisches Departement für
Umwelt, Verkehr, Energie und Kommunikation UVEK
Bundesamt für Strassen ASTRA

Zielerreichung:

The project achieved the targeted practice-oriented approaches for structural design and detailing of flexural strengthening layers made of TRC for bridge deck slabs, except for more detailed evaluations of TRC strengthening effects on shear and fatigue strength as well as on improvement of serviceability behavior, as associated literature data was missing.
A dimensioning approach for the anchorage of textiles embedded in mortar is presented in the report.
Possible integration in Swiss structural engineering customs and standards is achieved by referring to existing approaches frequently applied in practice (SIA 166 2004).

Folgerungen und Empfehlungen:

TRC represents a solid alternative for flexural strengthening of existing reinforced concrete elements. To further develop practical applications of TRC strengthening of slab elements, experimental studies that focus on efficiency of multiple textile layers should be conducted, in particular three and more textile layers and with PBO and basalt textiles, in bending but also for anchorages.
Theoretical investigations on the influence of the bond behavior between textile and surrounding mortar over the whole length of a flexurally strengthened slab element should be conducted. The proposed bond model for anchorages is a useful basis that should be extended to evaluating the structural behavior of TRC tension chords and their impact on the structural behavior of strengthened slabs, particularly w.r.t. improvements of serviceability behavior, and shear and fatigue strength of strengthened bridge deck slabs, the latter considering bond degradation due to reversed cyclic textile loading. These investigations should be combined with clear identification of governing control sections for structural dimensioning of TRC strengthening.
Normative guidelines should be made available (revision of SIA 166, for example). These require the consideration of conversion and material safety factors, as well as characteristic values for strain limits.
Determination of characteristic and design values for strain limits requires further investigations (for PBO and basalt textiles, in particular), representing identified lack of knowledge which will certainly be useful to the task group "textile reinforced concrete" of NK SIA 262, supporting its objectives.

Publikationen:

Muresan A. and Zwicky D. (2020). “Suitability Evaluation of Structural Analysis Approaches for Determining the Flexural Capacity of Reinforced Concrete Elements Strengthened with Textile-Reinforced Mortar”. Structural Engineering International, 30(4):545-550, DOI: 10.1080/10168664.2020.1776196 (published online July 14, 2020).

Muresan A.-M. and Zwicky D. (2018). “Dimensioning the flexural strengthening of concrete slabs with textile reinforced mortar – literature data evaluation”. In: Engineering the Past, to Meet the Needs of the Future, IABSE Conference, Copenhagen, June 25-27 2018, obtained Outstanding Young Engineer Contribution Award (one out of one).

Der Projektleiter/die Projektleiterin:

Name: Zwicky, Prof. Dr. Vorname: Daia

Amt, Firma, Institut: Institut für Bau- und Umwelttechnologien iTEC, Hochschule für Technik & Architektur HTA-FR

Unterschrift des Projektleiters/der Projektleiterin:

Schweizerische Eidgenossenschaft
Confédération suisse
Confederazione Svizzera
Confederaziun svizra

Eidgenössisches Departement für
Umwelt, Verkehr, Energie und Kommunikation UVEK
Bundesamt für Strassen ASTRA

FORSCHUNG IM STRASSENWESEN DES UVEK
Formular Nr. 3: Projektabschluss

Beurteilung der Begleitkommission:

Beurteilung:

Les objectifs initiaux de la recherche, assortis des observations et recommandations faites par la commission au fur et à mesure de l'avancement du projet, ont été atteints dans leur quasi-intégralité, notamment en termes
- de consolidation et d'évaluation de données et résultats expérimentaux issus de l'étude de la litérature,
- de développement et de calibration d'approches analytiques pour le dimensionnement, en évaluant leur adéquation avec les résultats expérimentaux,
- d'étude, incluant une phase expérimentale, d'un ancrage par adhérence des textiles et de la proposition d'une approche analytique afférente.

Umsetzung:

Le projet livre des résultats et des recommandations très utiles dans le cadre de l'utilisation de béton textile (notamment : fibres de carbone ou de PBO) aux fins de renforcement à la flexion de dalles unidirectionnelles de roulement.
Ces données concernent principalement
- le dimensionnement à l'état-limite ultime d'un renforcement à la flexion,
- le dimensionnement et la réalisation des ancrages de textiles au bord de la zone flexionnelle,
- les caractéristiques et propriétés des matériaux,
- les conditions et exigences pour la mise en oeuvre sur le chantier.

weitergehender Forschungsbedarf:

Le développement des applications du béton textile au renforcement d'éléments doit s'accompagner de recherches et d'essais complémentaires, notamment en ce qui concerne l'utilisation de couches multiples de textiles, l'influence de l'adhérence textile-mortier sur le comportement de l'élément renforcé, l'influence d'un renforcement à la flexion sur les résistances au cisaillement et à la fatigue ou encore l'évolution de la capacité de renforcement sous des cycles de chargement.

Einfluss auf Normenwerk:

Les résultats de la recherche peuvent être implémentés dans les documents normatifs et dans les directives, à l'exemple de la Norme SIA 166.

Der Präsident/die Präsidentin der Begleitkommission:

Name: Putallaz Vorname: Jean-Christophe

Amt, Firma, Institut: Ingénieur-conseil, Sion

Unterschrift des Präsidenten/der Präsidentin der Begleitkommission:

Forschung im Strassenwesen des UVEK: Formular 3 **Seite 3 / 3**